APÈNDIX

ELSEVIER

Neurobiology of Disease

www.elsevier.com/locate/ynbdi
Neurobiology of Disease 16 (2004) 92–97

Abnormal α-synuclein interactions with rab3a and rabphilin in diffuse Lewy body disease

E. Dalfó,[a,b] M. Barrachina,[a,b] J.L. Rosa,[c] S. Ambrosio,[c] and I. Ferrer[a,b,*]

[a] *Unitat de Neuropatologia Experimental, Departament de Biología Cellular i Anatomia Patològica, Hospitalet de Llobregat, Barcelona, Spain*
[b] *Institut de Neuropatologia, Hospital Universitari de Bellvitge, Hospitalet de Llobregat, Barcelona, Spain*
[c] *Unitat de Bioquímica, Departament de Ciències Fisiològiques II, Campus de Bellvitge, Universitat de Barcelona, Hospitalet de Llobregat, Barcelona, Spain*

Received 27 March 2003; revised 8 December 2003; accepted 7 January 2004

Available online 19 March 2004

The present study examines α-synuclein interactions with rab3a and rabphilin by antibody arrays, immunoprecipitation and pull-down methods in the entorhinal cortex of control cases and in diffuse Lewy body disease (LBD) cases. α-Synuclein immunoprecipitation revealed α-synuclein binding to rabphilin in control but not in LB cases. Immunoprecipitation with rab3a disclosed rab3a binding to rabphilin in control but not in LB cases. Moreover, rab3a interacted with high molecular weight (66 kDa) α-synuclein only in LB cases, in agreement with parallel studies using antibody arrays. Results were compared with pull-down assays using His_6/Flag-tagged rab3, rab5 and rab8, and anti-Flag immunoblotting. Weak bands of 17 kDa, corresponding to α-synuclein, were obtained in LB and, less intensely, in control cases. In addition, α-synuclein-immunoreactive bands of high molecular weight (36 kDa) were seen only in LB cases after pull-down assays with rab3a, rab5 or rab8. These findings corroborate previous observations showing rab3a–rabphilin interactions in control brains, and add substantial information regarding decreased binding of rab3a to rabphilin and increased binding of rab3a to α-synuclein aggregates in LB cases. Since, α-synuclein, rab3a and rabphilin participate in the docking and fusion of synaptic vesicles, it can be suggested that exocytosis of neurotransmitters may be impaired in LB diseases.
Published by Elsevier Inc.

Keywords: α-Synuclein; rab3a; rab5; rab8; Rabphilin; Lewy body disease

Introduction

α-Synuclein is a small, acidic protein containing 140 amino acids which is highly expressed in the brain and which is primarily localized in the presynaptic terminals (Clayton and George, 1998; Jakes et al., 1994; Lavedan, 1998; Ueda et al., 1993). α-Synuclein contains three modular domains, covering an amino-terminal lipid binding α-helix, an amyloid binding domain that encodes the non-Aβ component (NAC) of Alzheimer's disease amyloid plaques and a carboxyl-terminal acidic tail. This structure allows the molecule to exist as a disordered random coil in solution or as a α-helical structure after exposure to acidic phospholipid vesicles (Davidson et al., 1998). The protein associates with many substrates, including fatty acids and lipids, the dopamine transporter, synphilin, tau, microtubule-associated protein 2, tubulin, kinases and presynaptic vesicle membranes (Alim et al., 2002; Clayton and George, 1999; D'Andrea et al., 2001; Engelender et al., 1999; Ferrer et al., 2001; Jensen et al., 1999, 2000; Lee et al., 2001; Lücking and Brice, 2000; Payton et al., 2001; Sharon et al., 2001; Wakabayashi et al., 2002).

Several studies provide evidence that α-synuclein has a role in synaptic transmission. Marked reduction in the number of vesicles in the vesicle cluster, but not in the docking cluster, is found following anti-sense oligonucleotide α-synuclein ablation methods in fetal rat hippocampal cultures (Murphy et al., 2000). Recent findings have demonstrated that α-synuclein knock-out mice show a small reserve and/or resting pool of vesicles and increased synaptic depression during repetitive electrical stimulation (Cabin et al., 2002). These results support the notion that α-synuclein regulates synaptic vesicle mobilization at nerve terminals, particularly those in the reserve or resting pool (Abeliovich et al., 2000).

Synaptic vesicles contain several structural proteins, such as syntaxins, synaptobrevins/vesicle-associated membrane proteins (VAMP) and munc18/s1 (Bennet and Scheller, 1993; Jähn and Südhof, 1994; Söllner and Rothman, 1994; Südhof, 1995). In addition, several synaptic-associated proteins are involved in the trafficking and docking of synaptic vesicles, thus modulating docking and fusion of synaptic vesicles to the presynaptic membrane. Rab proteins are small guanine nucleotide exchanger (GTP–GDP-binding) proteins that are crucial for virtually every step in the intracellular membrane traffic. Rab3a is exclusively associated with synaptic vesicles and dissociates from the membrane vesicle during exocytosis (Fischer von Mollard et al., 1994; Lledó et al., 1994; Pfeffer, 1994; Simons and Zerial, 1993; Zerial and McBride, 2001). The GTP–GDP exchange modifies the affinity of rab protein for intracellular membranes and regulates vesicle trafficking (Fischer von Mollard et al., 1994). Synaptic vesicles contain three rab isoforms: rab3a is present in most if not all synapses in the rodent brain, whereas rab3b and rab3c are present in a subset of synapses (Fischer von Mollard et al., 1991,

* Corresponding author. Institut de Neuropatologia, Servei Anatomia Patològica, Hospital Universitari de Bellvitge, carrer Feixa LLarga sn, 08907 Hospitalet de Llobregat, Barcelona, Spain. Fax: +34-93-204-5065.
E-mail address: 8082ifa@comb.es (I. Ferrer).
Available online on ScienceDirect (www.sciencedirect.com.)

0969-9961/$ - see front matter. Published by Elsevier Inc.
doi:10.1016/j.nbd.2004.01.001

1994; Jähn and Südhof, 1994). Rab3 isoforms interact with different general rab-binding proteins and with at least two specific effector proteins: rabphilin-3A (Li et al., 1994; Shirataki et al., 1994) and Rim (Wang et al., 2002). Rab3a-null mutant worms (Nonet et al., 1997) and rab3a-null mice (Geppert et al., 1994) are viable, suggesting nonessential functions for rab3. Yet, *Caenorhabditis elegans* rab3-null mutants have fewer synaptic vesicles, especially near the active zone, but more synaptic vesicles at ectopic sites, suggesting that the transport of synaptic vesicles at the nerve terminal is impaired in the absence of rab3 (Nonet et al., 1997). And yet the morphology of the synapses appears to be normal in rab3a knock-out mice, although Ca^{2+}-triggered fusion is altered in the absence of rab3a (Geppert et al., 1994). It has been suggested that rab3a in mammals, unlike other rab proteins and rab3 in *C. elegans*, acts downstream from vesicle transport and vesicle docking at the active zone (Geppert et al., 1997).

Synaptic vesicles contain a peripheral membrane protein called rabphilin that binds selectively to the GTP-form of rab3a and rab3c (Li et al., 1994). The levels of rabphilin are greatly reduced in rab3a knock-out mice, supporting the notion that rabphilin interacts with rab3a in vivo (Geppert et al., 1994). Furthermore, overexpression of rabphilin in chromaffin cells strongly enhances transmitter release, indicating a functional role for rabphilin in exocytosis (Chung et al., 1995). However, rabphilin is not essential for the biological actions of rab3a, as no major synaptic deficits occur in rabphilin-null mice (Schlüter et al., 1999).

α-Synuclein is a major component of Lewy bodies and dystrophic neurites in Parkinson's disease (PD) and diffuse Lewy body disease (LBD) (Hashimoto and Masliah, 1999; Irizarry et al., 1998; Khale et al., 2002; Krüger et al., 2000; Lücking and Brice, 2000; Spillantini et al., 1997, 1998; Takeda et al., 1998; Wirdefeldt et al., 2001). Moreover, α-synuclein mutations are associated with familiar autosomic dominant PD (Krüger et al., 1998; Polymeropulos et al., 1997), thus indicating that modifications in α-synuclein may play a role in the pathogenesis of PD. Several studies have shown that α-synuclein aggregates in Lewy bodies (Baba et al., 1998; Lücking and Brice, 2000; Sulzer, 2001; Trojanowski and Lee, 1998), and that α-synuclein is abnormally phosphorylated (Fujiwara et al., 2002) and has a distinct structural conformation (Sharma et al., 2001) in PD. Yet, little is known about possible divergent properties of α-synuclein in Lewy body disorders regarding interactions of α-synuclein with selected synaptic proteins.

The present study is focused on the interactions of α-synuclein with rab3a and rabphilin in the healthy human brain and in the brain of cases with LBD. The identification of specific proteins that interact with α-synuclein may provide clues to learn about its normal function and to discover how those interactions may be affected in neurodegenerative diseases with impaired metabolism of α-synuclein.

Materials and methods

Tissue samples

Brain samples were obtained from the Institute of Neuropathology Brain Bank following the guidelines of the local ethics committee.

At autopsy, half of the brain was fixed in formalin, whereas the other half was cut in coronal sections 1 cm thick, frozen on dry ice and stored at −80°C until use. The entorhinal cortices of three cases (two men, one woman, aged 78, 79 and 76 years, respectively) with pure diffuse Lewy body disease (LB), as defined by large numbers of cortical Lewy bodies and dystrophic α-synuclein-immunoreactive neurites but not *tau* deposits or βA4 amyloid plaques, were used in the present study. Three age-matched brains with no neurological disease and normal neuropathological study were used as controls. The post-mortem delay was between 2 and 3 h in LB and control cases. Frozen samples from LB and control cases were processed in parallel.

Material and reagents

The Hypomatrix antibody array (Signal Transduction Antibody Array, Cat HM3000, Bionova, Madrid) consists of a membrane with 400 attached dots representing equal numbers of defined proteins.

Generation and purification of His_6/Flag-tagged rab3 and rab5 have been previously described (Rosa et al., 1996). His_6/Flag-tagged rab8 was generated and purified in a similar manner.

Rabbit polyclonal anti-α-synuclein antibody was from Chemicon (Pacisa Giralt, Barcelona). Antibodies used for immunoprecipitation assays, mouse monoclonal anti-α-synuclein and rabbit polyclonal anti-rab3a were from Neomarkers (Fremont, CA) and Calbiochem (Bionova, Madrid), respectively. The mouse monoclonal anti-rabphilin was from Transduction Laboratories (Lexington, KY), and the mouse monoclonal anti-rab3a antibody was provided by Dr. J. Blasi. Secondary antibodies and reagents were from DAKO (Barcelona). Flag antibodies were obtained from Sigma (Barcelona).

The specificity of the α-synuclein antibodies was tested by the observation of unique bands of 17 kDa in total brain homogenates of human cerebral cortex run in parallel with recombinant human α-synuclein (Calbiochem, Barcelona).

Antibody arrays

Samples of LB (1 g) were homogenized in 10 ml of PBS containing protease and phosphatase inhibitors (1 mM sodium orthovanadate, 10 μg/ml aprotinin, 1 mM phenylmethylsulfonyl fluoride) and centrifuged at 5000 rpm for 10 min at 4°C. The pellet was discarded and the supernatant was incubated with the membrane for 2 h at room temperature. Previously, the membranes were blocked with a solution containing 3% TBST-BSA for 1 h at room temperature. After washing with TBST, the membranes were incubated first with anti-α-synuclein antibodies (Chemicon) used at a dilution of 1/250 for 2 h at room temperature and then with streptavidin for 30 min, and developed with the ECL method (Amersham Biosciences, Madrid).

α-Synuclein immunoprecipitation and immunoblot

Samples (0.3 g) from LB and control cases were homogenized in a glass homogenizer in 10 volumes of ice-cold lysis buffer (Hepes 20 mM, pH 7.2, 1% Triton X-100, 1% sodium deoxycholate, 0.2% SDS, 150 mM NaCl, 1 mM sodium orthovanadate, 1 mM sodium fluoride, 10% glycerol, 10 μg/ml aprotinin, 1 mM phenylmethylsulfonyl fluoride) and centrifuged at 5000 rpm for 10 min at 4°C. The supernatant S1 was further centrifuged at 37,000 rpm for 1 h at 4°C to generate the supernatant S2. The S2 fraction was precleared with protein G-sepharose (Amersham) for 30 min at 4°C while shaking. Protein concentrations were determined using

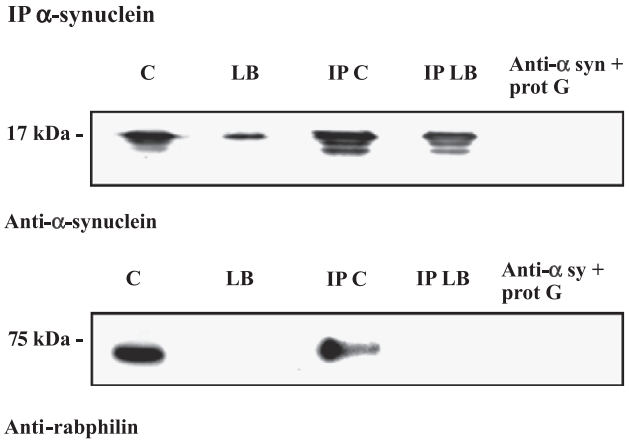

Fig. 1. Western blots of total homogenates from control (C) and diffuse Lewy body disease (LB) cases, and immunoprecipitates with α-synuclein in control (IPC) and diffuse Lewy body (IPLB) cases reveal specific bands at the appropriate molecular weight of 17 kDa, together with lower α-synuclein-immunoreactive bands. No immunoreaction is seen in the lane corresponding to anti-α-synuclein antibody and protein G-sepharose with no sample (anti-α-syn + prot G). The same membranes exposed to anti-rabphilin antibodies show strong bands at the appropriate molecular weight (75 kDa) in total homogenates and in immunoprecipitated samples from controls, but not from LB cases.

the Bradford method with bovine serum albumin as a standard. Equal aliquots of precleared P2 (1 mg) were incubated with anti-α-synuclein antibodies (Neomarkers) and 30 μl of 1:1 (v/v) protein G-sepharose beads for 4 h at 4°C. The immune complexes were collected by centrifugation and washed five times with a buffer containing 20 mM Tris, pH 7.5, 1 mM EDTA, 1 mM EGTA, 150 mM NaCl, 2 mM sodium orthovanadate, 10% glycerol and 1% Nonidet P-40 (Sigma, Madrid). The pellet was resuspended in sample buffer, and the immunocomplexes were processed for 12% SDS-PAGE electrophoresis and Western blot analysis. The membranes were incubated with anti-α-synuclein (Chemicon), anti-rab3a and anti-rabphilin antibodies used at dilutions of 1:2000, 1:1000 and 1:100, respectively. The protein bands were visualized using the ECL method (Amersham).

Rab3a immunoprecipitation and immunoblot

Rab3a immunoprecipitation assay was performed as described for rabconnectin (Nagano et al., 2002) with slight modifications. Briefly, 0.2 g of brain tissue from LB and control cases was homogenized with 7 volumes of immunoprecipitation buffer (20 mM Tris–HCl, pH 8.0, 1 mM EDTA, 150 mM NaCl and 1% Nonidet P-40) and then sonicated. After centrifugation at 5000 rpm for 10 min at 4°C, the pellet was discarded and the supernatant S1 was centrifuged at 37,000 rpm for 1 h at 4°C. The pellet was discarded, and the supernatant S2 was precleared with 40 μl protein G-sepharose for 30 min at 4°C. The protein concentration was determined by the Bradford method, and 2.5 mg of the precleared sample was incubated at 4°C overnight with the anti-rab3 antibody (Oncogene) immobilized with G-sepharose beads (60 μl). After washing, bound proteins were eluted by boiling the beads in SDS sample buffer without β-mercaptoethanol. The sample buffer consisted 3.8 ml of deionized water, 0.5 M Tris–HCl, pH 6.8, 1.0 ml, 0.8 ml glycerol, 1.6 ml SDS 10% (w/v) and 0.4 ml bromophenol blue 1% (w/v). Then the samples were subjected to 12% SDS-PAGE electrophoresis followed by Western blot analysis with anti-rab3a, anti-α-synuclein or anti-rabphilin antibodies used at dilutions of 1:1000, 1:2000 and 1:100, respectively. The protein bands were visualized using the ECL method.

Total homogenates and immunoprecipitated samples were processed in parallel with a lane containing the antibody used for immunoprecipitation and protein G-sepharose with no sample.

Rab pull-down assay

The S1 fraction obtained following the same protocol used for α-synuclein immunoprecipitation assays from LB and control cases was incubated with nickel-agarose containing 1 μg of His_6/Flag-tagged rab3, rab5 or rab8 for 1 h at 4°C while shaking. Following brief centrifugation (13,000 rpm, 30 s) of the reaction mixture, the precipitates were washed with PBS and resuspended with sample buffer.

Gels were transferred to nitrocellulose membranes (Biorad, Barcelona) and blotted with anti-FLAG (Rosa et al., 1996) at a dilution of 1:1000 or anti-α-synuclein antibodies (Chemicon) at a dilution of 1:2000. Total homogenates and pull-down samples were processed in parallel.

Results

Preliminary antibody arrays showed α-synuclein labeling of membrane dots, corresponding to rab3a, in brain homogenates of LB cases (data not shown), thus suggesting α-synuclein–rab3a binding in LB cases.

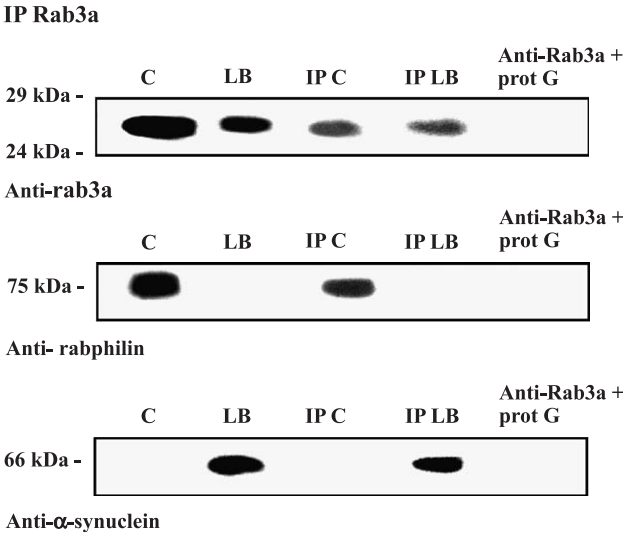

Fig. 2. Western blots of total homogenates from control (C) and diffuse Lewy body disease (LB) cases, and immunoprecipitates with rab3a in control (IPC) and diffuse Lewy body (IPLB) cases reveal specific bands at the appropriate molecular weight of about 26 kDa. No immunoreaction is seen in the lane corresponding to anti-α-rab3a antibody and protein G-sepharose with no sample (anti-rab3a + prot G). The same membranes exposed to anti-rabphilin antibodies show strong bands at the appropriate molecular weight (75 kDa) in total homogenates and in immunoprecipitated samples from controls, but not from LB cases. Yet, incubation with anti-α-synuclein antibodies discloses a different pattern. α-Synuclein-immunoreactive bands of high molecular weight (about 66 kDa) appear only in LB cases.

Immunoprecipitation studies were then carried out to corroborate these findings. α-Synuclein immunoprecipitation using the Neomarkers antibody was successful, as a single band of the appropriate molecular weight (17 kDa) appeared on Western blots processed with the anti-α-synuclein antibody from Chemicon in total homogenates and α-synuclein-immunoprecipitate samples. Moreover, no bands were seen in the lane corresponding to α-synuclein and protein G-sepharose alone (Fig. 1). Yet, visualization of rab3a, if present, was hampered in 12% SDS-PAGE gels by deposition of unspecific IgG light immunoglobulin binding at the same molecular weight (about 29 kDa) following incubation with anti-rab3a antibodies (data not shown). Incubation with anti-rabphilin antibodies revealed specific bands of 75 kDa in control but not in LB cases at the concentrations of protein and incubation times used in the present study (Fig. 1).

Immunoprecipitation with rabbit polyclonal anti-rab3a antibodies disclosed specific profiles in control and LB cases in total homogenates and following incubation with the monoclonal anti-rab3a antibody (Fig. 2). Incubation with anti-rabphilin showed specific bands (75 kDa) in control total homogenates and in control rab3a-immunoprecipitate samples, but not in LB cases, total homogenates and rab3a-immunoprecipitates (Fig. 2). These findings agree with previous observations showing interaction of rab3a and rabphilin in normal brains (Ostermeier and Brunger, 1999; Schlüter et al., 1999; Stahl et al., 1996).

In contrast, incubation with anti-α-synuclein antibodies showed immunoreactive bands only in LB cases; these unique bands had high molecular weights of about 66 kDa (Fig. 2). In every case, immunostaining was lacking in the lanes containing antibody and protein G-sepharose alone (Fig. 2).

To further demonstrate rab and α-synuclein interactions in control and LB cases, pull-down studies were carried out by using rab3a, rab5 and rab8. As seen in Fig. 3, pull-down assays were successful, as specific bands of Flag, which recognizes common sequences of rab proteins, were recovered in control and LB cases. In addition, pull-down assays revealed a band of 17 kDa in LB cases and, less intensely, in controls. Unspecific bands of 29 kDa were found in control and LB cases. Interestingly, high bands of about 36 kDa were seen only in LB cases following pull-down with all the rab proteins (Fig. 3).

The same results were obtained in three different experiments.

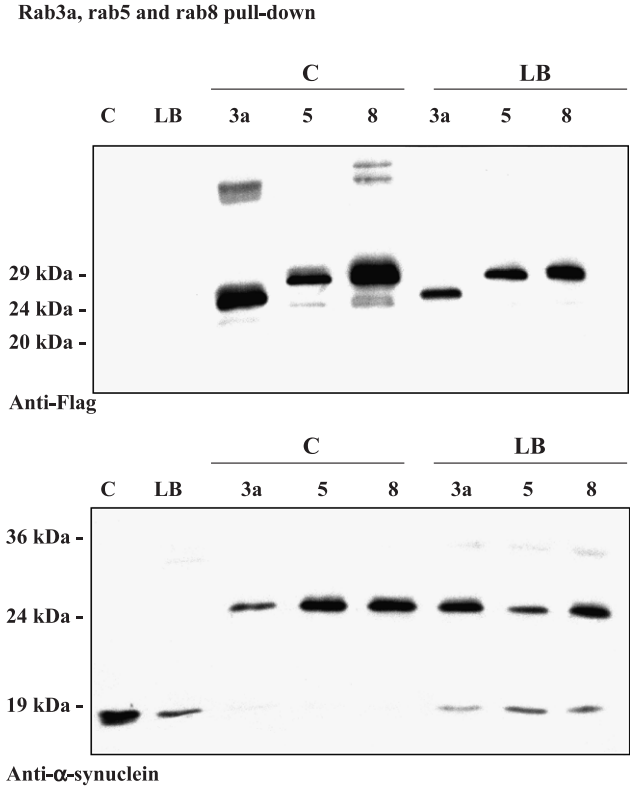

Fig. 3. Pull-down studies using His_6-tagged rab3, rab5 and rab8 in control (C) and diffuse Lewy body disease (LB) cases, and processed for anti-Flag immunoreactivity, show characteristic bands at the appropriate molecular weights, thus confirming successful experiment. The same membranes processed with anti-α-synuclein antibodies show weak bands of 17 kDa in LB and with less intensity in controls, but strong bands of high molecular weight (36 kDa) only in LB cases. Nonspecific bands of about 29 kDa, corresponding to IgG light immunoglobulin chain binding, are seen in control and LB cases. Membranes were processed in parallel with total homogenates of control and LB cases showing specific bands of 17 kDa in control and LB, and a weak band of 36 kDa in LB.

Discussion

The present results, based on immunoprecipitation and pull-down studies, have shown that α-synuclein interacts with rabphilin, and that rabphilin interacts with rab3a, in the normal brain. Although the interaction between rabphilin and rab3a has been previously reported (Ostermeier and Brunger, 1999; Schlüter et al., 1999; Stahl et al., 1996; Südhof, 1997), interactions of α-synuclein and rabphilin add complexity to this system at the presynaptic terminal.

Observations in rab3a and α-synuclein null-mice may add information regarding possible interactions among these proteins. α-synuclein knock-out mice show a small resting pool of synaptic vesicles that cannot efficiently replenish the ready releasable pool of vesicles following stimulation, thus leading to faster depletion of vesicles during prolonged repetitive stimulation, and, consequently, to increased synaptic depression during repetitive stimulation (Cabin et al., 2002). Interestingly, similar responses are seen in rab3a knock-out mice; the size of the readily releasable pool of vesicles is normal, whereas the Ca^{2+}-triggered fusion is altered in the absence of rab3a (Geppert et al., 1994). This suggests a similar or a collaborative function for these two proteins in the process of exocytosis. Direct interactions of soluble α-synuclein and rab3a are probably feeble in normal conditions, as very weak bands of α-synuclein immunoreactivity may be seen in rab pull-down studies. Since rab3a interacts with rabphilin, which in turn interacts with α-synuclein, it can be proposed that rabphilin may act as a bridge between rab3a and α-synuclein in the synaptic vesicle reserve pool. It can be argued that rabphilin depletion has no apparent effect on synaptic transmission (Schlüter et al., 1999). However, studies of prolonged repetitive stimulation in rabphilin null-mice are lacking, and therefore, a role for rabphilin in long-term exocytosis cannot be ruled out.

In contrast to control brains, α-synuclein in LB cases does not exhibit binding to rabphilin but rather to rab3a, according to combined α-synuclein and rab3a immunoprecipitation methods. This is further supported by rab pull-down studies in which α-synuclein binds to rab3a, thus corroborating preliminary studies using antibody arrays in LB cases. Pull-down studies have also extended α-synuclein interactions to other members of the GTP-binding protein Rab family, rab5 and rab8.

Rab3a interactions are also feeble with soluble α-synuclein as seen with weak bands of 17 kDa in LB cases. Yet pull-down studies have shown unique α-synuclein bands of high molecular weight (about 36 kDa). In addition, rab3a immunoprecipitation studies have demonstrated α-synuclein-immunoreactive bands of about 66 kDa. This is a very interesting point, as the high molecular bands herein observed may correspond to aggregated forms of α-synuclein reported in association with LB pathology (Campbell et al., 2000; Harding and Hallyday, 2001; Iwatsubo et al., 1996). Taken together, these combined methods point to the likelihood that α-synuclein interactions with rab3a and rabphilin in LB cases differ from those of α-synuclein in normal brain, and that these different interactions depend largely on the formation of α-synuclein aggregates.

The present model suggests rabphilin as a link between α-synuclein and rab3a, as both proteins interact with rabphilin in normal brain. This interaction is modified in pathological cases, as aggregated α-synuclein binds to rab3a, thereby preventing its binding with rabphilin. Such abnormal interaction, in turn, may affect the binding of rab3a to its molecular effector, rabphilin. Since rab3a is involved in the transport of synaptic vesicles in brain nerve terminals (Geppert et al., 1997; Leenders et al., 2001), it can be postulated that the docking function of rab3a is impaired in LB diseases.

It is clear that further studies are needed to demonstrate whether abnormal α-synuclein, rab3a and rabphilin interactions in LB diseases may undermine neurotransmitter exocytosis; yet the present observations provide insights for future research. In addition, it has been proposed that defective sequestration of dopamine into vesicles, leading to the generation of reactive oxygen species in the cytoplasm, is a key event in the demise of dopaminergic neurons in Parkinson's disease (Lotharius and Brundin, 2002). Since rab5 participates in endocytosis (Sung et al., 2001), abnormal binding of rab5 to α-synuclein aggregates, as observed in this study, may account for abnormal endocytosis of selected neurotransmitters in LB diseases as well.

Acknowledgments

This work was supported in part with FIS Grant OI020004, CICYT SAF2001-4681E and EU Project QLRI-CT2000-00066. We wish to thank T. Yohannan for editorial advice.

References

Abeliovich, A., Schmitz, Y., Farinas, I., Choi-Lundberg, D., Ho, W.H., Castillo, P.H., Shinsky, N., Verdugo, J.M., Armanini, M., Ryan, A., Inés, M., Phillips, H., Sulzer, D., Rosenthal, A., 2000. Mice lacking α-synuclein display functional deficits in the nigrostriatal dopamine system. Neuron 25, 239–252.

Alim, M.A., Hossain, M.S., Arima, K., Takeda, K., Izumiyama, Y., Nakamura, M., Kaji, H., Shinoda, T., Hisanaga, S., Ueda, K., 2002. Tubulin seeds alpha-synuclein formation. J. Biol. Chem. 18, 2112–2117.

Baba, M., Nakajo, S., Tu, P., Tomita, T., Nakaya, K., Lee, V.M.Y., Trojanowski, J.Q., Iwatsubo, T., 1998. Aggregation of α-synuclein in Lewy bodies of sporadic Parkinson's disease and dementia with Lewy bodies. Am. J. Pathol. 152, 879–884.

Bennet, M.K., Scheller, R.H., 1993. The molecular machinery for secretion is conserved from yeast to neurons. Proc. Natl. Acad. Sci. U. S. A. 90, 2559–2563.

Cabin, D.E., Shimazu, K., Murphy, D., Cole, N.B., Gottschalk, W., Mcllwain, K.L., Orrison, B., Chen, A., Ellis, C.E., Paylor, R., Lu, B., Nussbaum, R.L., 2002. Synaptic vesicle depletion correlates with attenuated synaptic responses to prolonged repetitive stimulation in mice lacking α-synuclein. J. Neurosci. 22, 8797–8807.

Campbell, B.C.V., Li, Q.-X., Culvenor, J.G., Jäkäla, P., Cappai, R., Beyreuther, K., Masters, C.L., McLean, C.A., 2000. Accumulation of insoluble α-synuclein in dementia with Lewy bodies. Neurobiol. Dis. 7, 192–200.

Chung, S.H., Takai, Y., Holz, R.W., 1995. Evidence that the rab3a-binding protein, rabphilin 3a, enhances regulated secretion. Studies in adrenal cromaffin cells. J. Biol. Chem. 270, 16714–16719.

Clayton, D.F., George, J.M., 1998. The synucleins: a family of proteins involved in synaptic function, plasticity, neurodegeneration and disease. Trends Neurosci. 21, 249–254.

Clayton, D.F., George, J.M., 1999. Synucleins in synaptic plasticity and neurodegenerative disorders. J. Neurosci. Res. 8, 120–129.

D'Andrea, M.R., Illyin, S., Plata-Salaman, C.R., 2001. Abnormal patterns of microtubule-associated protein-2 (MAP-2) immunolabeling in neuronal nuclei and Lewy bodies in Parkinson's disease substantia nigra brain tissues. Neurosci. Lett. 306, 137–140.

Davidson, W.S., Jonas, D.F., Clayton, D.F., George, J.M., 1998. Stabilization of α-synuclein secondary structure upon binding to synthetic membranes. J. Biol. Chem. 273, 9443–9449.

Engelender, S., Kaminski, Z., Guo, X., Sharp, A.H., Amaravi, R.K., Kleiderlein, J.J., Margolis, R.L., Troncoso, A.A., Lanahan, P.F., Worley, V.L., Dawson, T.M., Dawson, C.A., Ross, C.A., 1999. Synphilin-1 associates with alpha-synuclein and promotes the formation of cytosolic inclusions. Nat. Genet. 22, 110–114.

Ferrer, I., Blanco, R., Carmona, M., Puig, B., Borrachina, M., Gómez, C., Ambrosio, S., 2001. Active, phosphorylation-dependent mitogen-activated protein kinase (MAPK/ERK), stress-activated protein kinase/c-Jun N-terminal kinase (SAPK/JNK), and p38 kinase expression in Parkinson's disease and dementia with Lewy bodies. J. Neural Transm. 108, 1383–1396.

Fischer von Mollard, G., Südhof, T.C., Jan, R., 1991. A small GTP-binding protein dissociates from synaptic vesicles during exocytosis. Nature 349, 79–81.

Fischer von Mollard, G., Stahl, B., Li, C., Südhof, T.C., Jan, R., 1994. Rab proteins in regulated exocytosis. Trends Biochem. 19, 164–169.

Fujiwara, H., Hasegawa, M., Dohmae, N., Kawashima, A., Masliah, E., Goldberg, M.S., Shen, J., Takio, K., Iwatsubo, T., 2002. α-Synuclein is phosphorylated in synucleinopathy lesions. Nat. Cell. Biol. 4, 160–164.

Geppert, M., Bolshakov, V.Y., Siegelbaum, S.A., Takei, K., De Camilli, P., Hammer, R.E., Südhof, T.C., 1994. The role of Rab3A in neurotransmitter release. Nature 369, 493–497.

Geppert, M., Goda, Y., Stevens, C.F., Südhof, T.C., 1997. The small GTP-binding protein Rab3A regulates a late step in synaptic vesicle fusion. Nature 387, 810–814.

Harding, A.J., Hallyday, G.M., 2001. Cortical Lewy body pathology in the diagnosis of dementia. Acta Neuropathol. 102, 355–363.

Hashimoto, M., Masliah, E., 1999. Alpha-synuclein in Lewy body disease and Alzheimer's disease. Brain Pathol. 9, 707–720.

Irizarry, M.C., Growdon, W., Gómez-Isla, T., Newell, K., George, J.M., Clayton, D.F., Hyman, B.T., 1998. Nigral and cortical Lewy bodies in dystrophic nigral neurites in Parkinson's disease and cortical Lewy body disease contain α-synuclein immunoreactivity. J. Neuropathol. Exp. Neurol. 57, 334–337.

Iwatsubo, T., Yamaguchi, H., Fujimuro, M., Yokosawa, H., Ihara, Y., Trojanowski, J.Q., Lee, V.M., 1996. Purification and characterization of Lewy bodies from the brains of patients with diffuse Lewy body disease. Am. J. Pathol. 148, 1517–1529.

Jähn, R., Südhof, T.C., 1994. Synaptic vesicles and exocytosis. Annu. Rev. Neurosci. 17, 219–246.

Jakes, R., Spillantini, M.G., Goedert, M., 1994. Identification of two distinct synucleins from human brain. FEBS Lett. 345, 27–32.

Jensen, P.H., Hager, H., Nielsen, M.S., Hojrup, P., Gliemann, J., Jakes, R.,

1999. α-Synuclein binds to *tau* and stimulates the protein kinase A-catalyzed tau phosphorylation of serine residues 263 and 356. J. Biol. Chem. 36, 25481–25489.

Jensen, P.H., Islam, K., Kenney, J., Nielsen, M.S., Power, J., Gai, W.P., 2000. Microtubule-associated protein 1B is a component of cortical Lewy bodies and binds α-synuclein filaments. J. Biol. Chem. 275, 21500–21507.

Khale, P.J., Haass, C., Kretschmar, H.A., Neumann, M., 2002. Structure/function of α-synuclein in health and disease: rational development of animal models for Parkinson's and related diseases. J. Neurochem. 82, 449–457.

Krüger, R., Kuhn, W., Müller, T., Woitalia, D., Graber, M., Kosel, S., Przuntek, H., Epplen, J.T., Schols, L., Reiss, O., 1998. Ala30Pro mutation in the gene encoding α-synuclein in Parkinson's disease. Nat. Genet. 18, 106–108.

Krüger, R., Müller, T., Riess, O., 2000. Involvement of synuclein in Parkinson's disease and other neurodegenerative disorders. J. Neural Transm. 107, 31–40.

Lavedan, C., 1998. The synuclein family. Genome Res. 8, 871–880.

Lee, F.S.J., Liu, Z.B., Pristupa, H.B., Niznik, H.B., 2001. Direct binding and functional coupling of α-synuclein to the dopamine transporters accelerate dopamine-induced apoptosis. FASEB J. 15, 916–926.

Leenders, M.A.G., Lopes da Silva, F.H., Ghijsen, E.J.M.W., Verhage, M., 2001. Rab3A is involved in transport of synaptic vesicles to the active zone in mouse brain nerve terminals. Mol. Biol. Cell. 12, 3095–3102.

Li, C., Takei, K., Geppert, M., Daniell, L., Stenius, K., Chapman, E.R., Jahn, R., De Camilli, P., Südhof, T.C., 1994. Synaptic targeting of rabphilin-3A, a synaptic vesicle Ca^{2+}/phospholipid-binding protein, depends on Rab3A/C. Neuron 13, 885–898.

Lledó, P.M., Johannes, L., Vernier, P., Zorec, R., Darchen, F., Vincent, J.D., Henry, J.P., Mason, W.T., 1994. Rab3 proteins: key players in the control of exocytosis. Trends Neurosci. 17, 426–432.

Lotharius, J., Brundin, P., 2002. Pathogenesis of Parkinson's disease: dopamine, vesicles and α-synuclein. Nat. Rev. 3, 1–11.

Lücking, C.B., Brice, A., 2000. Alpha-synuclein and Parkinson's disease. Cell. Mol. Life Sci. 57, 1894–1908.

Murphy, D.D., Rueter, S.M., Trojanowski, J.Q., Lee, V.M., 2000. Synucleins are developmentally expressed, and α-synuclein regulates the size of presynaptic vesicular pool in primary hippocampal neurons. FEBS Lett. 470, 93–95.

Nagano, F., Kawabe, H., Nakanishi, H., Shinoara, M., Deguchi-Tawarada, M., Takeuchi, M., Sasaki, T., Takai, Y., 2002. Rabconnectin-3, a novel protein that binds both GDP/GTP exchange protein and GTPases-activating protein for rab3 small G protein family. J. Biol. Chem. 277, 9629–9632.

Nonet, M.L., Stauton, J.E., Kilgard, M.P., Fergestad, T., Hartwieg, E., Horvitz, H.R., Jorgersen, E.M., Meyer, B.J., 1997. *Caenorhabditis elegans* rab-3 mutant synapses exhibit impaired function and are partially depleted of vesicles. J. Neurosci. 17, 8061–8063.

Ostermeier, C., Brunger, T.A., 1999. Structural basis of Rab effector specificity: crystal structure of the small G protein Rab3a complexed with the effector domain of rabphilin-3A. Cell 96, 363–374.

Payton, J.E., Perrin, R.J., Clayton, D.F., George, J.M., 2001. Protein–protein interactions of α-synuclein in brain homogenates and transfected cells. Mol. Brain Res. 95, 138–145.

Pfeffer, S.R., 1994. Rab GTPases: master regulators of membrane trafficking. Curr. Opin. Cell Biol. 6, 522–526.

Polymeropulos, M.H., Lavedant, C., Leroy, E., Ide, S.E., Dehejia, A., Dutra, A., Pike, B., Root, H., Rubenstein, J., Boyer, R., Stenroos, E.S., Chandrasekharappa, S., Athanassiadou, A., Papapetropoulos, T., Johnson, W.G., Lazzani, A.M., Duvoisin, R.C., Di Iorio, G., Golbe, Ll., Nussbaum, R.L., 1997. Mutations in the α-synuclein gene identified in families with Parkinson's disease. Science 276, 2045–2047.

Rosa, J.L., Casaroli-Marano, R.P., Buckler, A.J., Vilaró, S., Barbacid, M., 1996. p619, a giant protein related to the chromosome condensation regulator RCC1, stimulates guanine nucleotide exchange on ARF1 and Rab proteins. EMBO J. 15, 4262–4273.

Schlüter, O.M., Schnell, E., Verhage, M., Tzonopoulos, T., Nicoll, R.A., Janz, R., Malenka, R.C., Geppert, M., Südhof, T.C., 1999. Rabphilin knock-out mice reveal that rabphilin is not required for rab3 function in regulating neurotransmitter release. J. Neurosci. 19, 5834–5846.

Sharma, N., McLean, P.J., Kawamata, H., Irizarry, M.C., Hyman, B.D., 2001. Alpha-synuclein has an altered conformation and shows a tight intermolecular interaction with ubiquitin in Lewy bodies. Acta Neuropathol. 102, 329–334.

Sharon, R., Goldberg, M.S., Bar-Josef, I., Betensky, R.A., Shen, J., Selkoe, D.J., 2001. α-Synuclein occurs in lipid-rich high molecular weight component, binds fatty acids, and shows homology to the fatty acid-binding proteins. Proc. Natl. Acad. Sci. U. S. A. 98, 9110–9115.

Shirataki, H., Yamamoto, T., Hagi, S., Miura, H., Oishi, H., Jin-no, Y., Senbonmatsu, T., Takai, Y., 1994. Rabphilin-3a is associated with synaptic vesicles in a manner independent of Rab3a. J. Biol. Chem. 269, 32717–32720.

Simons, K., Zerial, M., 1993. Rab proteins and the road maps for intracellular transport. Neuron 11, 789–799.

Söllner, T., Rothman, J.E., 1994. Neurotransmission: harnessing fusion machinery at the synapse. Trends Neurosci. 17, 3444–3447.

Spillantini, M.G., Schmidt, M.L., Lee, V.M.Y., Trojanowski, J.Q., Jakes, R., Goedert, M., 1997. α-Synuclein in Lewy bodies. Nature 388, 839–840.

Spillantini, M.G., Growther, R.A., Jakes, R., Hasegawa, M., Goedert, M., 1998. α-Synuclein in filamentous inclusions of Lewy bodies from Parkinson's disease and dementia with Lewy bodies. Proc. Natl. Acad. Sci. U. S. A. 95, 6469–6473.

Stahl, B., Chou, J.H., Li, C., Südhof, C., Jahn, R., 1996. Rab3 reversibly recruits rabphilin to synaptic vesicles by a mechanism analogous to raf recruitment by ras. EMBO J. 15, 1799–1809.

Südhof, T.C., 1995. The synaptic vesicle cycle: a cascade of protein interactions. Nature 375, 645–653.

Südhof, T.C., 1997. Function of Rab3 GTP–GDP exchange. Neuron 18, 519–522.

Sulzer, D., 2001. α-Synuclein and cytosolic dopamine: stabilizing a bad situation. Nat. Med. 7, 1280–1282.

Sung, J.Y., Kim, J., Paik, S.R., Park, J.H., Ahn, Y.S., Chung, K.C., 2001. Induction of neuronal death by Rab5A-dependent endocytosis of α-synuclein. J. Biol. Chem. 276, 27441–27448.

Takeda, A., Hashimoto, M., Mallory, M., Sundsumo, M., Hioner, W., Hansen, L., Masliah, E., 1998. Abnormal accumulation of NACP/α-synuclein in neurodegenerative disorders. Am. J. Pathol. 152, 367–372.

Trojanowski, J.Q., Lee, V.M.Y., 1998. Aggregation of neurofilament and α-synuclein in Lewy bodies: implications for the pathogenesis of Parkinson disease and Lewy body dementia. Arch. Neurol. 55, 151–152.

Ueda, K., Fukushima, H., Masliah, E., 1993. Molecular cloning of cDNA encoding an unrecognized component of amyloid in Alzheimer disease. Proc. Natl. Acad. Sci. U. S. A. 90, 11282–11286.

Wakabayashi, K., Engelender, S., Tanaka, Y., Yoshimoto, M., Mori, F., Tsuji, S., Ross, C.A., Takahashi, H., 2002. Immunocytochemical localization of synphilin-1, an α-synuclein-associated protein, in neurodegenerative disorders. Acta Neuropathol. 103, 209–214.

Wang, Y., Liu, X., Biederer, T., Südhof, T.C., 2002. A family of RIM-binding proteins regulated by alternative splicing. Implications for the genesis of synaptic active zones. Proc. Natl. Acad. Sci. U. S. A. 99, 14464–14469.

Wirdefeldt, K., Bogdanovic, N., Westerberg, L., Payami, H., Schalling, M., Murdoch, G., 2001. Expression of α-synuclein in the human brain: relation to Lewy body disease. Mol. Brain Res. 92, 58–65.

Zerial, M., McBride, H., 2001. Rab proteins as membrane organizers. Nat. Rev. 2, 107–119.

ABNORMAL α-SYNUCLEIN INTERACTIONS WITH RAB PROTEINS IN α-SYNUCLEIN A30P TRANSGENIC MICE.

E. Dalfó (1), T. Gómez-Isla, MD, PhD (4), J.L. Rosa, PhD (3), M. Nieto Bodelón (4), M. Cuadrado Tejedor, PhD (4), M. Barrachina, PhD (2), S. Ambrosio, PhD (3), I. Ferrer, MD, PhD (1, 2)

Unitat de Neuropatologia Experimental, Departament de Biologia Cel.lular i Anatomia Patològica, Universitat de Barcelona (1); Institut de Neuropatologia, Servei Anatomia Patològica, Hospital Universitari de Bellvitge, Hospitalet de Llobregat, Barcelona (2); Unitat de Bioquímica, Departament de Ciències Fisiològiques II, Universitat de Barcelona, Hospitalet de Llobregat (3); Departamento de Neurología, Universidad de Navarra, 31008 Pamplona, Navarra (4); Spain

Corresponding author: Prof. I. Ferrer, Institut de Neuropatologia, Servei Anatomia Patològica, Hospital Universitari de Bellvitge, carrer Feixa Llarga sn, 08907 Hospitalet de Llobregat, Spain.
E-mail: 8082ifa@comb.es
or
iferrer@csub.scs.es

Publicat a **Journal of Neuropathology and Experimental Neurology**, Vol. 63 No. 4, April-2004, pp. 302-313.

ABSTRACT

Mutation A30P in the α-synuclein gene is a cause of familial Parkinson's disease. Transgenic mice expressing wild mouse and mutant human A30P α-synuclein, Tg5093 mice (Tg), show a progressive motor disorder characterized by tremor, rigidity and dystonia, accompanied by accumulation of α-synuclein in the soma and neurites, and by a conspicuous gliosis beginning in the hippocampal formation at the age of 7-8 months and spreading throughout the CNS. Impaired short-term changes in synaptic strength have also been documented in hippocampal slices from Tg5093 mice. α-synuclein aggregates of about 34 and 70 kDa, in addition to the band of 17 kDa, corresponding to the molecular weight of α-synuclein, were recovered in the PBS-soluble fraction of brain homogenates from Tg5093 mice but not from brain samples from age-matched wildtype littermates (W). MPTP-treated Tg and W mice produced α-synuclein aggregates in the PBS-, deoxycholate- and SDS-soluble fractions. Aggregates of α-synuclein, although with different molecular weight, were also observed in rotenone-treated Tg and W mice. Pull-down studies with members of the Rab protein family have shown that α-synuclein from Tg5093 mice interacts with Rab3a, Rab5 and Rab8. This binding is not due to the amount of α-synuclein (levels of which are higher in Tg5093 mice) and it is not dependent on the amount of Rab protein used in the assay. Rather, α-synuclein interactions with Rab proteins are due to mutant α-synuclein as demonstrated in Rab pull-down assays with recombinant of wildtype and mutant A30P human α-synuclein. Since Rab3a, Rab5 and Rab8 are important proteins involved in synaptic vesicle trafficking and exocytosis at the synapse, vesicle endocytosis, and trans-Golgi transport, respectively, it can be suggested that these functions are impaired in Tg5093 mice. This rationale is consistent with previous data showing that short-term hippocampal synaptic plasticity is altered and that α-synuclein accumulates in the cytoplasm of neurons in Tg5093 mice.

Keywords: α-synuclein, Parkinson's disease, Rab3a, Rab5, Rab8, synapse, MPTP, rotenone

INTRODUCTION

α-synuclein is a highly conserved protein of 140 amino acid residues which is abundant in presynaptic terminals (1-5). α-synuclein has been linked to the pathogenesis of Parkinson's disease (PD) with the discovery of missense mutations (A53T and A30P) in several families affected by early onset familial PD (6-8), a feature that has been demonstrated in sporadic and familial PD (9-12). In addition, α-synuclein is implicated in Diffuse Lewy Body Disease (DLBD), and it accumulates in Lewy bodies and aberrant neurites in both familial and sporadic PD and in DLBD (2, 5, 6, 13-17). Although the mechanism of Lewy body formation is not completely known, self-aggregating α-synuclein is the major subunit protein of the filamentous lesions observed in PD (18). Moreover, oxidative dimer formation is the critical rate-limiting step for α-synuclein fibrillogenesis in PD (19).

Transgenic α-synuclein mice manifest variable phenotypes and pathologies which are dependent not only on the type of α-synuclein but also on the characteristics of the transgen promoter (20, 21). Transgenic mice expressing mutant A53T or mutant A30P human α-synuclein show somal and neuritic accumulations of α-synuclein in the brain, accompanied by variable motor deficits (22-24). Expression of non-mutant mice α-synuclein and mutant A30P human α-synuclein in Tg5093 mice results in a progressive motor disorder associated with aberrant expression of the protein in the cell soma and with progressive gliosis, but without specific anatomical or biochemical disruption of the nigrostriatal dopaminergic system (25). Finally, Tg5093 mice exhibit altered short-term hippocampal synaptic plasticity (26).

Mice lacking α-synuclein display functional deficits and abnormal synaptic function in the nigrostriatal dopaminergic system (27). Furthermore, recent studies have demonstrated a small reserve and/or resting pool of vesicles and increased synaptic depression during repetitive electrical stimulation in α-synuclein knock-out mice (28), thus supporting the notion that α-synuclein regulates synaptic vesicle mobilization at nerve terminals, particularly those in the reserve or resting pool (27).

Considering these data, it is feasible that mutant α-synuclein may have several implications in pathology. On the one hand, mutated α-synuclein may have properties of solubility and a capacity to form aggregates that differ from those of wild α-synuclein. On the other hand, and more important in the present context, interactions of α-synuclein with proteins linked with exocytosis and/or vesicle recycling, and with neurotransmission, may be impaired by mutant α-synuclein.

Rab proteins are a large family of GTPases that control membrane transport and cell trafficking by shifting between GTP-and GDP-bound conformations (29). Rab3a is enriched on synaptic vesicles and dissociates from synaptic vesicles during exocytosis (30, 31). Studies in mutants have shown that Rab3a regulates neurotransmitter release during the late steps in exocytosis (32-35). Rab5 participates in ligand sequestration at the plasma membrane and in the motility of endosomes, whereas Rab8 controls the traffic between the trans-Golgi network and the plasma membrane (29).

Exposure to the environmental toxin 1-methyl-4-phenyl-1,2,3,6-tetrahydropyridine (MPTP) causes selective dopaminergic neuron degeneration

in the substantia nigra and loss of dopaminergic terminals in the striatum (36, 37). Chronic exposure to the pesticide rotenone, a highly selective complex I inhibitor, can reproduce anatomical, neurochemical and neuropathological features of PD in rodents, including accumulation of α-synuclein in nigral dopaminergic neurons (38).

In the present study, we have examined modifications in α-synuclein solubility and aggregation in transgenic mice expressing wild mouse α-synuclein and in mutant A30P human α-synuclein mice (Tg5093 line: Tg) when compared with age-matched wildtype controls (W). We have also tested the hypothesis that A30P mutant human α-synuclein may have abnormal interactions with members of the Rab family, including Rab3a, Rab5 and Rab8, thus potentially compromising synaptic vesicle trafficking, endocytosis, and α-synuclein transport. Tg5093 and wild mice have also been subjected to MPTP or to rotenone treatment to study the effects on A30P α-synuclein solubility, aggregation and interaction with Rab target proteins.

MATERIALS AND METHODS

Transgenic mice

The generation of Tg5093 mice has been previously described (25). In brief, the cDNA encoding human α-synuclein containing the A30P mutation was expressed in C57B/6jxSJL F3 hybrid mice using a hamster prion protein (PrP) cosmid vector, in which the PrP open reading frame (ORF) was replaced with the human α-synuclein ORF. This vector has been previously shown to drive transgene product expression throughout neurons in the brain, including the substantia nigra and other vulnerable neuronal populations in Lewy body disorders. Subsequent generations of mice were produced using C57B/6jxSJL F1 breeders.

The Tg5093 mouse line demonstrates several features of the human synucleinopathies, including a progressive motor disorder characterized by an age-dependent appearance of unilateral and then bilateral tremor, rigidity and dystonic posturing affecting limbs and axial muscles, accumulation of α-synuclein in the soma and proximal neurites of neurons, and ubiquitin immunoreactive astrocytes. However, certain details of these features are distinct from those in humans, most conspicuously the finding that the nigrostriatal dopaminergic system is preserved in these animals and that they do not develop Lewy body-like neuronal inclusions (25). The most prominent neuropathological feature of these mice is an age-related gliosis beginning in the hippocampal formation at the age of 7-8 months that spreads to the cerebral cortex, subcortical regions, brain stem and spinal cord. In addition, impaired short-term changes in synaptic strength have been documented in hippocampal slices from Tg5093 mice (26).

MPTP and rotenone treatment

Groups of Tg and W mice at ages 3-4 months (MPTP or saline) and 6-10 months (rotenone or DMSO) received one of the following chronic treatment regimens: group I (n=4), daily intraperitoneal injection of 16 mg/Kg MPTP-HCl in 0.9% saline for 5 consecutive days (total dose = 80 mg/Kg); group II (n=4), daily intraperitoneal injection of 0.9% saline alone for 5 consecutive days; group III (n=3) intraperitoneal injections of rotenone in DMSO twice a week for 3 consecutive weeks (total dose = 0.250 mg/Kg); and group IV (n=2), intraperitoneal injections of DMSO alone twice a week for 3 consecutive weeks. Animals were sacrificed at 7 and 30 days after the last injection of MPTP or rotenone, respectively. All the animals included in this study were asymptomatic.

Tissue Preparation

Mice were sacrificed under CO_2 and the entire brain was removed and snap-frozen in dry ice.

α-synuclein solubility and aggregation

α-synuclein aggregates were isolated as previously described for glial citoplasmic inclusions in Multiple System Atrophy, with slight modifications (39, 40). Brain samples (0.06 g) from treated and non-treated Tg and W mice were homogenized in a glass homogenizer in 500 μl of ice-cold PBS^+ (sodium phosphate buffer, pH 7.0, plus protease inhibitors), sonicated and centrifuged

5,000 rpm at 4ºC for 10 min. The pellet was discarded and the resulting supernatant was ultracentrifuged at 37,000 rpm at 4ºC for 1 h. The supernatant (S2) was kept as the PBS-soluble fraction. The resulting pellet was re-suspended in a solution of PBS, pH 7.0, containing 0.5% sodium deoxycholate, 1% Triton and 0.1% SDS, and was ultracentrifuged at 37,000 rpm at 4ºC for 1 h. The resulting supernatant (S3) was kept as the deoxycholate-soluble fraction. The corresponding pellet was re-suspended in a solution of SDS 2% in PBS and maintained at room temperature for 2 h. Immediately afterwards, the samples were centrifuged at 37,000 rpm at 25ºC for 1 h, and the resulting supernatant (S4) was the SDS-soluble fraction. Finally, the corresponding pellet was re-suspended in a solution of 5% SDS-urea 8 M and incubated by rotation O/N at room temperature. After centrifugation at 37,000 rpm at 25ºC for 1 h, the pellet was discarded and the supernatant (S5) was kept as the urea-soluble fraction.
Equal amounts of each fraction were mixed with reducing sample buffer and processed for 10% SDS-PAGE electrophoresis and Western blot analysis. The membranes were incubated with anti-α-synuclein (Chemicon, Pacisa Giralt, Barcelona) at a dilution of 1:1,000. The protein bands were visualized by the ECL method (Amersham, Barcelona).

Rab pull-down assay

Brain tissue (0.06 g) from treated and non-treated Tg and W mice was homogenized in 500 μl of buffer composed of 20 mM Tris-HCl, pH 8.0, 1 mM EDTA, 150 mM NaCl and 1% Nonidet P-40, and then sonicated. After centrifugation at 5,000 rpm for 10 min at 4ºC, the pellet was discarded and the supernatant S1 was ultracentrifuged at 37,000 rpm for 1 h at 4ºC. The pellet was discarded, and the supernatant S2 was pre-cleared with 30 μl of nickel beads. The resulting fraction was divided into three equal volumes (200 μl) which were incubated with previously blocked nickel beads and 1 μg of His_6/Flag-tagged Rab3, Rab5 or Rab8 for 1 h at 4ºC while shaking. The generation and purification of His_6/Flag-tagged Rab3, Rab5 and Rab8 have been previously described (41). Following centrifugation at 12,000 rpm for 30 sec, the precipitates were washed with ice-cold PBS and re-suspended with sample buffer.
Gels were transferred to nitrocellulose membranes (Biorad, Barcelona) and blotted with anti-Flag (Sigma, Barcelona) at a dilution of 1:1,000, anti-α-synuclein (Chemicon) at a dilution of 1:1,000, or anti-β-actin (Sigma) used at a dilution of 1:1,000. Total homogenates and pull-down samples were processed in parallel. A lane containing the S2 fraction and only nickel beads was used as a control for the pull-down assay.

Rab5 pull-down with recombinant α-synuclein

Recombinant 61-140 wildtype α-synuclein and mutant A30P human α-synuclein (Calbiochem, Barcelona), both at 1 mg/ml in PBS, were incubated with previously blocked nickel beads and different amounts of His_6/Flag-tagged Rab5 (10 μg, 20 μg, 50 μg) for 1 h while shaking. Following centrifugation at 12,000 rpm for 30 sec, the precipitates were washed with ice-cold PBS and re-suspended with sample buffer.

Gels were transferred to nitrocellulose membranes (Biorad) and blotted with anti-Flag (Sigma) at a dilution of 1:1,000 or anti-α-synuclein (Chemicon) at a dilution of 1:1,000. 20 μg of non-pulled human recombinant α-synucleins, wildtype and A30P mutant forms, were processed in parallel. A lane containing only the recombinant A30P mutant α-synuclein (20 μg) and nickel beads was used as a control for the pull-down assay.

Rab3a immunoprecipitation and immunoblot

Brain tissue (0.2 g) from Tg and W mice was homogenized with 7 volumes of immunoprecipitation buffer (20 mM Tris/Cl pH: 8.0, 1 mM EDTA, 150 mM NaCl and 1% Nonidet p-40) and then sonicated. After centrifugation at 5,000 rpm for 10 min at 4ºC, the pellet was discarded and the supernatant S2 was pre-cleared with 40 µl protein G-sepharose for 30 min at 4ºC. The protein concentration was determined by the Bradford method, and 2.5 mg of the pre-cleared sample was incubated at 4ºC overnight with anti-Rab3 antibody (Santa Cruz Biotechnology, Madrid) immobilized with G-sepharose beds (60 µl). After washing, bound proteins were eluted by boiling the beads in SDS sample buffer without mercaptoethanol. The sample buffer consisted of 3.8 ml of de-ionized water, 0.5 M Tris-HCl, pH: 6.8, 1.0 ml, 0.8 ml glycerol, 1.6 ml SDS 10% (w/v) and 0.4 ml bromophenol blue 1% (w/v). Then the samples were subjected to 12% SDS-PAGE electrophoresis followed by Western blot analysis with anti-Rab3a (monoclonal, Dr. J Blasi), anti-α-synuclein (Neomarkers, Bionova, Barcelona), anti-rabphilin (Transduction Lab, Lexington, KY) and anti-β actin (Sigma). The anti-α-synuclein antibody recognizes human α-synuclein but not mouse α-synuclein. The antibodies were used at dilutions of 1:1,000, 1:2,000, 1:100 and 1:1,000, respectively. The protein bands were visualized ith the ECL method (Amersham Biosciences). Total homogenates were processed in parallel with a lane containing the antibody used for immunoprecipitation and protein G-sepharose with no sample.
In addition, Rab3a immunoprecipitation assays were carried out with normal human cerebral cortex obtained at post-mortem following generous donation for research to the Institute of Neuropathology and brain bank of Bellvitge, and according to the recomendations of the local Ethic Committee. Rab3a immunoprecipitation was carried out with Rab3a antibody (Calbiochem) 2 µg/ml. Western blot analysis was conducted with Rab3a monoclonal antibody (Dr. J. Blasi) used at a dilution of 1:100 and with the monoclonal anti-α-synuclein antibody (Neomarkers) used at a dilution of 1:100.

RESULTS

α-synuclein aggregates

α-synuclein (17 kDa) was mainly recovered in the PBS-soluble fraction, whereas small amounts were recovered in the deoxycholate- (DC-) and SDS-soluble fractions in non-treated Tg and W mice (Fig. 1). The amount of α-synuclein was higher in Tg, as previously described in these mice (25). In addition, α-synuclein-immunoreactive bands of about 34 and 70 kDa were observed only in the PBS-soluble fractions of Tg mice. No similar bands were recognized in non-treated W mice (Fig. 1). Interestingly, MPTP-treated Tg and W mice produced α-synuclein aggregates distributed in the PBS-, DC- and SDS-soluble fractions. Aggregates were also observed in rotenone-treated Tg and W mice. Yet the molecular weight of the bands differed in the two experimental models. Several bands of variable molecular weight were found in the PBS-soluble fraction in rotenone-treated mice whereas bands of 45 kDa were recovered in MPTP-treated mice. Bands of about 66 kDa in the PBS-, DC- and SDS-soluble fractions were equally observed in MPTP-treated and rotenone-treated Tg and W mice (Fig. 1). No bands were found in the urea-soluble fraction in non-treated and treated Tg and W mice (Fig. 1). The same results were observed in several consistent blots.

Rab pull-down assays

Pull-down assays were carried out by using His_6/Flag-tagged Rab3a, Rab5 and Rab8 in brain samples of non-treated, MPTP-treated, and rotenone-treated α-synuclein Tg and W mice.

α-synuclein, manifested as a band of about 17 kDa with specific antibodies that recognize human and mice α-synuclein, was recovered in total brain homogenates of W and Tg non-treated mice. Pull-down assays showed α-synuclein specific bands of 17 kDa in pulled samples of non-treated Tg mice. No such bands were observed in pulled samples of non-treated W mice. No signal was obtained in the lane corresponding to the S2 fraction incubated with nickel beads but without His_6/Flag-tagged Rabs (Fig. 2). The same membranes were immunostained for Flag that recognizes common sequences of Rab proteins. Flag immunoreactivity in Rab3a, Rab5 and Rab8 pull down-assays was similar in W and Tg mice (Fig. 2), thus showing that differences in α-synuclein immunoreactivity were not due to different Rab protein loading in pull-down assays. Control of protein loading was tested by incubating the membranes with anti-β-actin. In spite of similar protein loading in the lanes corresponding to W and Tg total brain homogenates, as revealed by the β-actin signal, the amount of α-synuclein was higher in Tg than in W mice (Fig. 2).

Rab pull-down assays in MPTP- and rotenone-treated rats showed α-synuclein specific bands of 17 kDa in pulled samples of MTPT-treated and rotenone-treated Tg mice, but not in pulled samples of MPTP-treated and rotenone-treated W mice. No signal was obtained in the lane corresponding to the S2 fraction incubated with nickel beads but without His_6/Flag-tagged Rabs (Fig. 3).

To demonstrate that the bindings observed in these pull-down experiments were specifically due to mutated α-synuclein and to rule out the possibility that the amount of protein was not responsible for the differences between W and Tg mice, Rab5 pull-down assays were carried out using recombinant wildtype and recombinant A30P mutant α-synuclein. Pull-down assays incubated with the anti-α-synuclein antibody revealed a specific band of 17 kDa in non-pulled total homogenates of W and Tg mice, and in Rab5-pulled samples with recombinant mutant A30P α-synuclein. However, no bands were observed in Rab5-pulled samples with recombinant wildtype α-synuclein (Fig. 4). Yet Flag-immunoreactive bands were recovered equally in His_6/Flag-tagged Rab5 pull-down assays with recombinant wildtype and A30P mutant α-synucleins (Fig. 4).

Rab3 immunoprecipitation assays

To control and corroborate the results of pull-down assays, Rab3a immunoprecipitation studies were carried out in Tg and W mice. Samples were run in parallel with total brain homogenates of Tg and W mice. Rab3a-pulled samples immunoblotted for anti-Rab3a showed similar bands at the appropriate molecular weight in TG and W samples. Yet α-synuclein was recovered only in pulled Tg samples and tTg. Since this antibody used does not recognize mouse synuclein, no signals were recovered in W samples (Fig. 5). Membranes immunoblotted for rabphilin disclosed similar immunoreactive bands in Tg and W samples, thus indicating Rab3a/rabphilin binding.

To test that Rab3a/α-synuclein interactions in Tg mice were due to mutant /α-synuclein and not to wildtype human synuclein, immunoprecipitation studies with Rab3a were carried out in control human cortex. Rab-3a was recovered in immunoprecipitated, but α-synuclein was not recovered in Rab3a-immunoprecipiated samples although it was present in total brain homogenates (Fig. 6).

DISCUSSION

The present study has shown α-synuclein aggregates in brain homogenates of Tg5093 mice expressing wild mouse α-synuclein and mutant A30P human α-synuclein (Tg), but not in brain homogenates of age-matched non-transgenic mice (W). Modifications of α-synuclein solubility have been previously observed in human Lewy body diseases and these are recapitulated in transgenic mouse models (42-46). Changes in α-synuclein solubility and α-synuclein aggregation occur in brain homogenates in W and Tg mice treated with MPTP or with rotenone. These results complement previous observations showing α-synuclein up-regulation and increased capacity of α-synuclein aggregation in target neurons following MPTP treatment in mice and baboons (47, 48). Similarly, the present results further support α-synuclein aggregation following rotenone exposure (49).

Rab3a is exclusively associated with synaptic vesicles and dissociates from membranes during exocytosis (29, 30, 50-52). Rab3a null-mutant *Caenorhabditis elegans* (33) and Rab3a-null mice (32) are viable, suggesting non-essential functions for Rab3. Yet Ca^{2+}-triggered fusion of vesicles is altered in the absence of Rab3 in mice (32), whereas Rab3-null worm mutants have fewer synaptic vesicles, especially near the active zone, but more synaptic vesicles at ectopic sites (33), suggesting that the transport of synaptic vesicles at the nerve terminal is impaired in the absence of Rab3a. Recent data indicate that Rab3a regulates a late step in synaptic vesicle fusion (34).

The present study has also shown that mutant A30P human α-synuclein, but not wildtype α-synuclein, interacts with Rab proteins Rab3a, Rab5 and Rab8 as seen in Rab pull-down assays. This binding is not dependent on the amount of Rab protein used in the assay, as Rab5 pull-down with recombinant wildtype and with mutant A30P α-synuclein shows α-synuclein immunoreactivity not only with the mutant form, but also Flag immunoreactivity (which recognizes Rabs) in the lanes corresponding to wildtype and mutant α-synuclein. Nor is binding of mutant α-synuclein with Rab dependent on the amount of α-synuclein, as Rab5 pull-down assays with increasing doses of recombinant wildtype and mutant α-synucleins demonstrates Rab5 binding only with the mutant form even in conditions in which the system is saturated for mutant α-synuclein.

Pull-down studies have been corroborated by Rab3a immunoprecipitation assays, in which α-synuclein from Tg mice, but not α-synuclein from W mice, interacts with Rab3a. Yet Rab3a interacts with rabphilin, as it is well documented (53, 54). Finally, Rab3a/α-synuclein interactions are not simply related with the presence of human α-synuclein because no Rab3a/α-synuclein binding has been previously reported in normal conditions and non similar interactions have been here observed in Rab3a immunoprecipitation assays with control human cortical samples. Therefore, combined pull-down and immunoprecipitation methods demonstrate that mutant synuclein interacts with Rabs in Tg mice.

These data, together with observations derived from α-synuclein and Rab3a mutants, permit us to delineate a scenario in which α-synuclein and Rab3a play complementary and independent functions in the regulation of synaptic vesicle trafficking. Lack of α-synuclein or Rab3a is associated with impaired synaptic vesicle transport, whereas mutated α-synuclein results in abnormal binding with

Rab3a, thus presumably contributing to abnormal synaptic function. In this line, it is worth stressing that short-term hippocampal synaptic plasticity is altered in the transgenic mice used in the present study (26).
Defective sequestration of dopamine into vesicles, leading to the generation of reactive oxygen species in the cytoplasm, has been suggested as playing a role in the degeneration of dopaminergic neurons (55). Furthermore, cells expressing mutant α-synuclein are more sensitive to a variety of toxic insults (56) and may cause increased susceptibility to dopaminergic toxicity (11, 12, 57). Recent studies have shown that Rab5 participates in the endocytosis of α-synuclein and dopamine (58). Binding of mutant α-synuclein to Rab5, as observed in the present study, may account for abnormal endocytosis of selected neurotransmitters, and may increase dopamine toxicity in substantia nigra pars compacta neurons.
Rab8 participates in the trans-Golgi network-plasma membrane traffic (29). Therefore, it can be suggested that mutant α-synuclein binding to Rab8 may have consequences on α-synuclein traffic in the cytosol. An interesting aspect in several transgenic models, including the present transgenic mice (25), is the translocation of mutant α-synuclein to the cytosol. Although several factors may be involved in this process, abnormal interactions of mutant α-synuclein with Rab8 may account for α-synuclein deposition in the cytoplasm.
Finally, in contrast to their effects on α-synuclein solubility and aggregation, MPTP and rotenone do not have any effect on the interaction of α-synuclein with Rab proteins. It is not the effect of the toxicity but rather the nature of α-synuclein (mutant α-synuclein in the present paradigm) that gears the fate of α-synuclein binding with Rab3a, Rab5 and Rab8.
Yet we have recently shown that Tg5093 mice are more vulnerable than littermate controls to MPTP in a dose-dependent manner. Tg mice exhibit higher mortality rates, more accentuated loss of TH positive neurons in the substantia nigra pars compacta, and more pronounced decrease in striatal dopamine and TH levels when compared to age-matched littermate controls. These findings support the idea that over-expression of mutant A30P α-synuclein in Tg5093 mice increases the vulnerability of their dopaminergic nigrostriatal system to MPTP (unpublished observations). The mechanism by which over-expression of A30P α-synuclein in Tg5093 mice enhances their sensitivity to MPTP remains to be elucidated. It has been previously shown that the selective toxicity of MPP+ for DA neurons derives, at least in part, from its high affinity for the DA transporter (DAT). Intraneuronally, MPP+ can be sequestered into synaptic vesicles by the vesicular monoamine transporter (VMAT), and sequestration into vesicles decreases MPP+ toxicity by preventing its interaction with the mitochondria. According to this model, cellular vulnerability to MPTP in Tg5093 mice might occur if level and activity of DAT or VMAT were altered in these mice. We have previously demonstrated that VMAT-2 binding is unaffected in the striatum of Tg5093 mice (25). It is possible, though, that a compromise at other steps of membrane trafficking pathways could account for the increased dopaminergic neuron vulnerability seen in these mice. In this sense, the abnormal interaction between α-synuclein and Rab proteins in Tg5093 mice described here could potentially interfere with sequestration of MPP+ into synaptosomal vesicles, enhancing its direct interaction with mitochondria and thus its toxicity. In addition, the finding that these abnormal interactions occur at presymptomatic clinical stages preceding

the motor dysfunction that characterizes the phenotype of Tg5093 mice suggests that they could potentially underlie the clinical and electrophysiological abnormalities found in this transgenic line.

ACKNOWLEDGEMENTS

This work was supported in part by grants FIS PI020004, C03-006 and G03-1XXX and EC DIADEM QLRT-2000-02362. We thank T. Yohannan for editorial assistance.

FIGURE LEGENDS

Fig 1: α-synuclein solubility and aggregation in brain homogenates of non-treated, MPTP-treated and rotenone-treated mice, and blotted for α-synuclein. Samples from two groups of mice were processed in parallel, Tg5093 mice expressing wildtype mouse α-synuclein and mutated human A30P α-synuclein (Tg), and wildtype littermates of transgenic mice expressing only wildtype mouse α-synuclein (W). Several fractions were recovered in the different lanes: PBS-, deoxycholate- (DC-), SDS- and urea- (U-)soluble fractions. In addition to the larger amount of PBS-, DC- and SDS-soluble α-synuclein of 17 kDa in Tg compared with W mice, bands of high molecular weight of 34 kDa and about 70 kDa are detected in the PBS-soluble fraction of Tg mice. Treatment with MPTP results in the formation of high molecular weight α-synuclein aggregates (45 and 66 kDa) and modifications in α-synuclein solubility in both W and Tg mice. Treatment with rotenone results in the formation of different synuclein aggregates which are multiple in the PBS-soluble fraction and of about 50 kDa in the PBS-, DC- and SDS-soluble fractions in both W and Tg mice. In no case was α-synuclein recovered in the urea-soluble fraction.

Fig. 2: Pull-down studies using His_6/Flag-tagged Rab3, Rab5 and Rab8 in non-treated wildtype littermates (W) and Tg5093 (Tg) mice, and processed for α-synuclein immunoreactivity, show characteristic bands of 17 kDa in Tg mice, while no bands are present in W mice. Membranes were processed in parallel with total brain homogenates (tW and tTg) showing specific bands of 17 kDa in W and Tg mice. These homogenates were also processed with nickel beads alone as a control for the pull-down experiment, and no specific bands were observed. The same membranes were incubated with anti-Flag antibodies that showed similar bands in pull-down samples obtained from W and Tg mice, thus indicating similar Rab protein content in pulled W and Tg samples. Finally, control of protein loading in the lanes corresponding to the total brain homogenates was tested by incubating the membranes with antibodies to β-actin.

Fig. 3: Pull-down studies using His_6/Flag-tagged Rab3, Rab5 and Rab8 in MPTP- and rotenone-treated wildtype littermates (W) and Tg5093 (Tg) mice, and processed for α-synuclein immunoreactivity, show characteristic bands of 17 kDa in MPTP-treated and rotenone-treated Tg mice, while no bands are present in W mice. Membranes were processed in parallel with total brain homogenates (tW and tTg) showing specific bands of 17 kDa in W and Tg mice. These homogenates were also processed with nickel beads alone as a control for the pull-down experiment, and no specific bands were observed.

Fig. 4: Pull-down studies using His_6/Flag-tagged Rab5, and recombinant wildtype and A30P mutant human α-synuclein, and processed with α-synuclein antibodies show bands of 17 kDa in lanes with A30P mutant α-synuclein. No bands were observed in the pull-down assay with wildtype α-synuclein. The same membranes processed for anti-Flag show similar bands at the appropriate molecular weights in W and Tg mice. Increasing amounts (10, 20 and 50μg) of

α-synuclein (wildtype and A30P-mutant) were processed with His_6/Flag-tagged Rab5. 20 μg of wildtype and A30P mutant α-synuclein without Rab5 were used as a control of the pull-down assay. Early saturation explains similar signals for the different doses of α-synuclein in this particular assay.

Fig. 5: Rab3a immunoprecipitation assay and Western blot (ipRab3a) from Tg and W mice processed in parallel with total brain homogenates (tTg and tW) show specific Rab3a bands at the appropriate molecular weigth. No signal is observed in the lane corresponding to anti-Rab3a and protein G sepharose (Rab3a + protG). Yet, α-synuclein is found only in Tg mice, thus indicating Rab3a/α-synuclein binding in Tg but not in W mice. In contrast, rabphilin immunoreactivy is recovered in total homogenates and immunoprecipited samples from both Tg and W mice. Finally, protein loading in total homogenates was tested with β-actin.

Fig. 6: Rab3a immunoprecipitation assay and Western blot in human cortex (ipC) discloses specific Rab3a bands at the appropriate molecular weigth in total homogenates (tC) and Rab3a-immunoprecipitate sample (ipC). No signal is observed in the lane corresponding to anti-Rab3a and protein G sepharose (Rab3a + protG). α-synuclein is found only in total homogenates but not in ipC samples.

REFERENCES

1. George J M, Jin H, Woods WS, Clayton DF. Characterization of a novel protein regulated during the critical period for song learning in the zebra finch. Neuron 1995;15:361-372

2. Iwai A, Masliah E, Yoshimoto M, Ge N, Flanagan L, de Silva HA, Kittel A, Saitoh T. The precursor protein of non-A beta component of Alzheimer's disease amyloid is a presynaptic protein of the central nervous system. Neuron 1995;14:467-475

3. Withers GS, George JM, Banker GA, Clayton DF. Delayed localization of synelfin (synuclein, NACP) to presynaptic terminals in cultured rat hippocampal neurons. Brain Res Dev Brain Res 1997;99:87-94

4. Clayton DF, George JM. The synucleins: a family of proteins involved in synaptic function, plasticity, neurodegeneration and disease. Trends Neurosci 1998;21:249-254

5. Lykkebo S, Jensen PH. Alpha-synuclein and presynaptic function. NeuroMolecular Med 2002;2:115-129

6. Polymeropoulos MH, Lavedan C, Leroy E, Ide SE, Dehejia A, Dutra A, Pike B, Root H, Rubenstein J, Boyer R, Stenroos ES, Chandrasekharappa S, Athanassiadou A, Papapetropoulos T, Johnson WG, Lazzarini AM, Duvoisin RC, Di Iorio G, Golbe LI, Nussbaum RL. Mutation in the alpha-synuclein gene identified in families with Parkinson's disease. Science 1997;276:2045-2047

7. Kruger R, Kuhn W, Muller T, Woitalla D, Graeber M, Kosel S, Przuntek H, Epplen JT, Schols L, Riess O. Ala30Pro mutation in the gene encoding alpha-synuclein in Parkinson's disease. Nat Genet 1998;18:106-108

8. Polymeropoulos MH. Autosomal dominant Parkinson's disease and alpha-synuclein. Ann Neurol 1998;44:S63-64

9. Goldberg MS, Lansbury PT. Is there a cause-and-effect relationship between α-synuclein fibrillization and Parkinson's disease? Nat Cell Biol 2000;2:115-119

10. Galvin JE, Lee VM, Trojanowski JQ. Synucleinopathies: clinical and pathological implications. Arch Neurol 2001;58:186-190

11. Goedert M. Alpha-synuclein and neurodegenerative diseases. Nat Rev Neurosci 2001;2:492-501

12. Goedert M. Parkinson's disease and other alpha-synucleinopathies. Clin Chem Lab Med 2001;39:308-312

13. Ueda K, Fukushima H, Masliah E, Xia Y, Iwai A, Yoshimoto M, Otero DA, Kondo J, Ihara Y, Saitoh T. Molecular cloning of cDNA encoding an

unrecognized component of amyloid in Alzheimer disease. Proc Natl Acad Sci USA1993;90:11282-11286

14. Irizarry MC, Kim TW, McNamara M, Tanzi RE, George JM, Clayton DF, Hyman BT. Characterization of the precursor protein of the non-A beta component of senile plaques (NACP) in the human central nervous system. J Neuropathol Exp Neurol 1996;55:889-895

15. Spillantini MG, Schmidt ML, Lee VM, Trojanowski JQ, Jakes R, Goedert M. Alpha-synuclein in Lewy bodies. Nature 1997;388:839-840

16. Wakabayashi K, Matsumoto K, Takayama K, Yoshimoto M, Takahashi H. NACP, a presynaptic protein, immunoreactivity in Lewy bodies in Parkinson's disease. Neurosci Lett 1997;239:45-48

17. Gomez-Tortosa E, Newel K, Irizarry MC, Sanders JL, Hyman BT. Alpha-synuclein immunoreactivity in dementia with Lewy bodies: morphological staging and comparison with ubiquitin immunostaining. Acta Neuropathol 2000;99:352-357

18. Giasson BI, Uryu K, Trojanowski JQ, Lee VM. Mutant and wild type human alpha-synucleins assemble into elongated filaments with distinct morphologies in vitro. J Biol Chem 1999;274:7619-7622

19. Krishnan S, Chi EY, Wood SJ, Kendrick BS, Li C, Garzón-Rodriguez W, Wypych J, Randolph TW, Narhi LO, Biere AL, Citron M, Carpenter JF. Oxidative dimer formation is the critical rate-limiting step for Parkinson's disease α-synuclein fibrillogenesis. Biochemistry 2003;42:829-837

20. Kahle PJ, Haas C, Kretzschmar HA, Neumann M. Structure/function of synuclein in health and disease: rational development of animal models for Parkinson's and related diseases. J Neurochem 2002;82:449-457

21. Jellinger KA. Experimental models of synucleinopathies. In: Dickson D Edit. Neurodegeneration: The molecular pathology of dementia and movement disorders. Basel: ISN Neuropathol Press, 2003:215-223

22. Kahle PJ, Neumann M, Ozmen L, Haass C. Physiology and pathophysiology of alpha-synuclein. Cell culture and transgenic animal models based on a Parkinson's disease-associated protein. Ann N Y Acad Sci 2000;920:33-41

23. Masliah E, Rockenstein E, Veinbergs I, Mallory M, Hashimoto M, Takeda A, Sagara Y, Sisk A, Mucke L. Dopaminergic loss and inclusion body formation in alpha-synuclein mice: implications for neurodegenerative disorders. Science 2000;287:1265-1269

24. van der Putten H, Wiederhold KH, Probst A, Barbieri S, Mistl C, Danner S, Kauffmann S, Hofele K, Spooren WP, Ruegg MA, Lin S, Caroni P, Sommer B,

Tolnay M, Bilbe G. Neuropathology in mice expressing human alpha-synuclein. J Neurosci 2000;20:6021-6029

25. Gomez-Isla T, Irizarry MC, Mariash A, Cheung B, Soto O, Schrump S, Sondel J, Kotilinek L, Day J, Schwarzschild MA, Cha JH, Newell K, Miller DW, Ueda K, Young AB, Hyman BT, Ashe KH. Motor dysfunction and gliosis with preserved dopaminergic markers in human alpha-synuclein A30P transgenic mice. Neurobiol Aging 2003;24:245-258

26. Steidl JV, Gomez-Isla T, Mariash A, Ashe KH, Boland LM. Altered short-term hippocampal synaptic plasticity in mutant synuclein transgenic mice. Neuroreport 2003;14:219-223

27. Abeliovich A, Schmitz Y, Farinas I, Choi-Lundberg D, Ho WH, Castillo PE, Shinsky N, Verdugo JM, Armanini M, Ryan A, Hynes M, Phillips H, Sulzer D, Rosenthal A. Mice lacking alpha-synuclein display functional deficits in the nigrostriatal dopamine system. Neuron 2000;25:239-252

28. Cabin, DE, Shimazu K, Murphy D, Cole NB, Gottschalk W, McIlwain KL, Orrison B, Chen A, Ellis CE, Paylor R, Lu B, Nussbaum RL. Synaptic vesicle depletion correlates with attenuated synaptic responses to prolonged repetitive stimulation in mice lacking alpha-synuclein. J Neurosci 2002;22:8797-8807

29. Zerial M, McBride H. Rab proteins as membrane organizers. Nat Rev Mol Cell Biol 2001;2:107-117

30. Fischer von Mollard G, Stahl B, Li C, Südhof TC, Jahn R. Rab proteins in regulated exocytosis. Trends Biochem Sci 1994;19:164-168

31. Jahn R, Südhof TC. Synaptic vesicles and exocytosis. Annu Rev Neurosci 1994;17:219-246

32. Geppert M, Bolshakov VY, Siegelbaum SA, Takei K, De Camilli P, Hammer RE, Sudhof TC. The role of Rab3A in neurotransmitter release. Nature 1994;369:493-497

33. Nonet M L, Staunton J.E, Kilgard MP, Fergestad T, Hartwieg E, Horvitz HR, Jorgensen EM, Meyer BJ. Caenorhabditis elegans rab-3 mutant synapses exhibit impaired function and are partially depleted of vesicles. J Neurosci 1997;17: 8061-8073

34. Geppert M, Goda Y, Stevens CF, Südhof TC. The small GTP-binding protein Rab3A regulates a late step in synaptic vesicle fusion. Nature 1997;387:810-814

35. Geppert M, Südhof TC. Rab3 and synaptotagmin: The yin and yang of synaptic membrane fusion. Annu Rev Neurosci 1998;21:75-95

36. Langston JW, Ballard P, Tetrud JW, Irwin I. Chronic parkinsonism in humans due to a product of meperidine-analog synthesis. Science 1993;219:979-980

37. Przedborski S, Vila M. The 1-methyl-4-phenyl-1,2,3,6-tetrahydropyridine mouse model: a tool to explore the pathogenesis of Parkinson's disease. Ann N Y Acad Sci 2003;991:189-98

38. Betarbet R, Sherer TB, MacKenzie G, Garcia-Osuna M, Panov AV, Greenamyre JT. Chronic systemic pesticide exposure reproduces features of Parkinson's disease. Nat Neurosci 2000;3:1301-1306

39. Dickson DW, Liu W, Hardy J, Farrer M, Mehta N, Uitti R, Mark M, Zimmerman T, Golbe L, Sage J, Sima A, D'Amato C, Albin R, Gilman S, Yen SH. Widespread alterations of alpha-synuclein in multiple system atrophy. Am J Pathol 1999;155:1241-1251

40. Gai WP, Pountney DL, Power JH, Li QX, Culvenor JG, McLean CA, Jensen PH, Blumbergs PC. Alpha-synuclein fibrils constitute the central core of oligodendroglial inclusion filaments in multiple system atrophy. Exp Neurol 2003;181:68-78

41. Rosa JL, Casaroli-Marano RP, Buckler AJ, Vilaro S, Barbacid M. p619, a giant protein related to the chromosome condensation regulator RCC1, stimulates guanine nucleotide exchange on ARF1 and Rab proteins. Embo J 1996;15: 4262-4275

42. El-Agnaf OM, Jakes R, Curran MD, Wallace A. Effects of the mutations Ala30 to Pro and Ala53 to Thr on the physical and morphological properties of alpha-synuclein protein implicated in Parkinson's disease. FEBS Lett 1998;440:67-70

43. Conway KA, Harper JD, Lansbury PT. Accelerated in vitro fibril formation by a mutant alpha-synuclein linked to early-onset Parkinson disease. Nat Med 1998;4:1318-1320

44. Kahle PJ, Neumann M, Ozmen L, Muller V, Odoy S, Okamoto N, Jacobsen H, Iwatsubo T, Trojanowski JQ, Takahashi H, Wakabayashi K, Bogdanovic N, Riederer P, Kretzschmar HA, Haass C. Selective insolubility of alpha-synuclein in human Lewy body diseases is recapitulated in a transgenic mouse model. Am J Pathol 2001;159:2215-2225

45.Conway KA, Harper JD, Lansbury PT. Fibrils formed in vitro from alpha-synuclein and two mutant linked to Parkinson's disease are typical amyloid. Biochemistry 2000;39:2552-2563

46. Li J, Uversky VN, Fink AL. Effect of familial Parkinson's disease point mutations A30P and A53T on the structural properties, aggregation, and fibrillation of human α-synuclein. Biochemistry 2001;40:11604-11613

47. Kowal NW, Hantraye P, Brouillet E, Beal MF, McKee AC, Ferrante RJ. MPTP induces synuclein aggregation in the substantia nigra of baboons. NeuroReport 2000;11:211-213

48. Vila M, Vukosavic S, Jackson-Lewis V, Neystat M, Jakowec M, Przedborski S. Alpha-synuclein up-regulation in substantia nigra dopaminergic neurons following administration of the parkinsonian toxin MPTP. J Neurosci 2000;74:721-729

49. Sherere TH, Kim JH, Betarbet R, Greenamyre JT. Subcutaneus rotenone exposure causes highly selective dopaminergic degeneration and α-synuclein aggregation. Exp Neurol 2002;179:9-16

50. Simons K, Zerial M. Rab proteins and the road maps for intracellular transport. Neuron 1993;11:789-799

51. Lledo PM, Johannes L, Vernier P, Zorec R, Darchen F, Vincent JD, Henry JP, Mason WT. Rab3 proteins: key players in the control of exocytosis. Trends Neurosci 1994;17:426-432

52. Pfeffer SR. Rab GTPases: master regulators of membrane trafficking. Curr Opin Cell Biol 1994;6:522-526

53. Li C, Takei K, Geppert M, Daniell L, Stenius K, Chapman ER, Jahn R, De Camilli P, Südhof TC. Synaptic targeting of rabphilin-3A, a synaptic vesicle Ca^{2+}/phospholipid-binding protein, depends on Rab3A/C. Neuron 1994;13:885-898

54. Shirataki H, Yamamoto T, Hagi S, Miura H, Oishi H, Jin-no Y, Senbonmatsu T, Takai Y. Rabphilin-3a is associated with synaptic vesicles in a manner independent of Rab3a. J Biol Chem 1994;269:32717-32720

55. Lotharius J, Brundin P. Pathogenesis of Pakinson's disease: dopamine, vesicles and α-synuclein. Nature Rev 2002;3:1-11

56. Lee M, Hyun D, Halliwell B, Jenner P. Effect of the overexpression of wild-type or mutant alpha-synuclein on cell susceptibility to insult. J Neurochem 2001;76:998-1009

57. Tabrizi SJ, Orth M, Wilkinson JM, Taanman JW, Warner TT, Cooper JM, Schapira AH. Expression of mutant alpha-synuclein causes increased susceptibility to dopamine toxicity. Hum Mol Genet 2000;9:2683-2689

58. Sung JY, Kim J, Paik SR, Park JH, Ahn YS, Chung KC. Induction of neuronal death by Rab5A-dependent endocytosis of synuclein. J Biol Chem 2001;276:27441-27448

α-synuclein aggregates

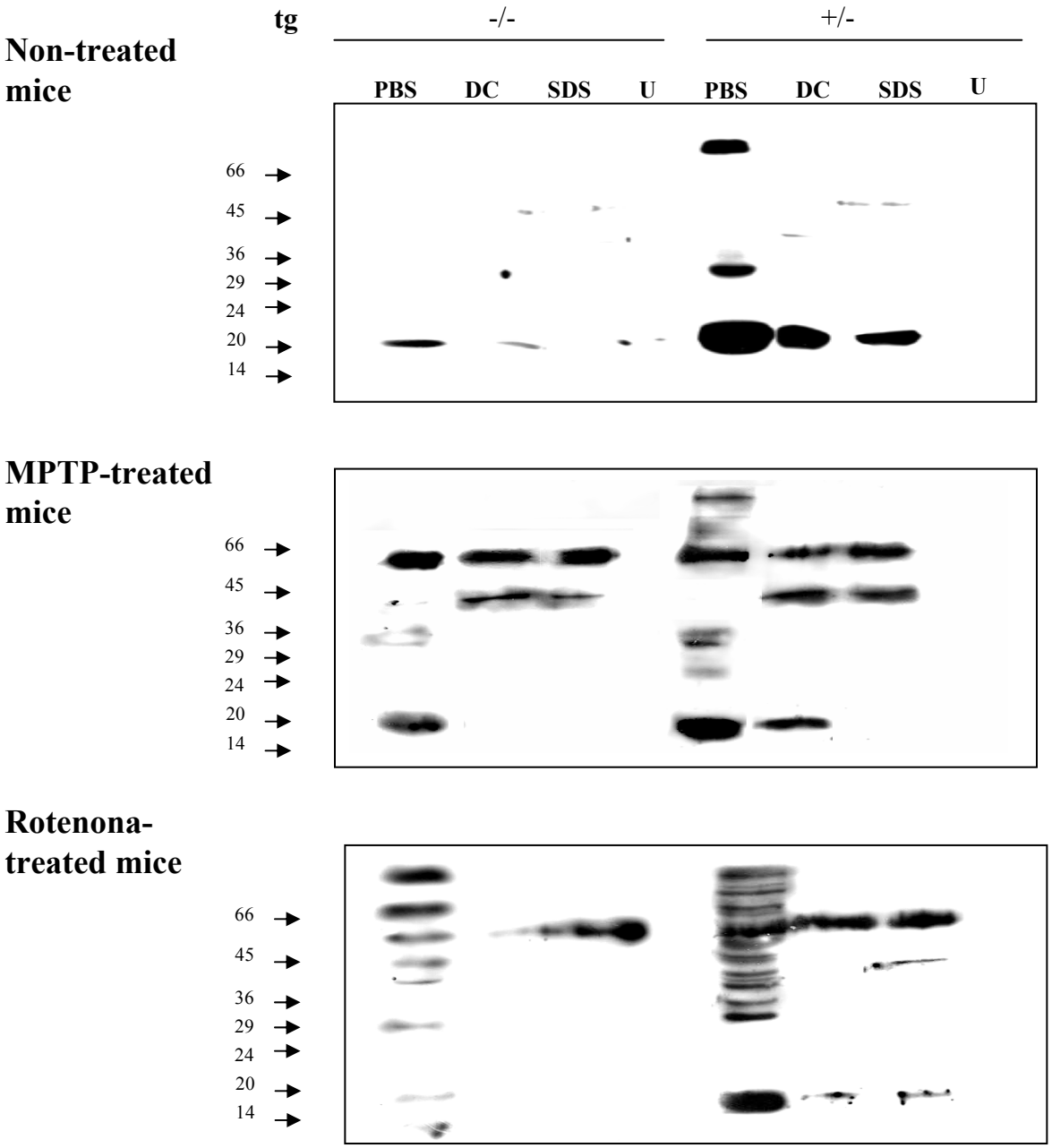

Rab pull-down in non=treated transgenic mice

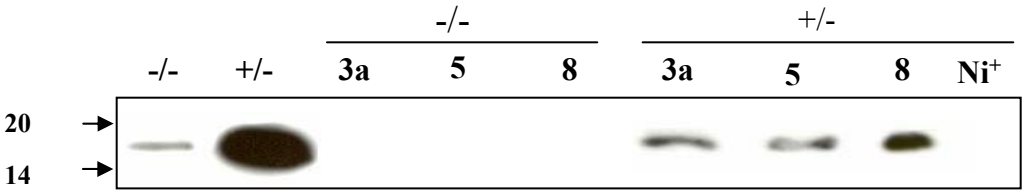

IB anti-α-syn 1:1000

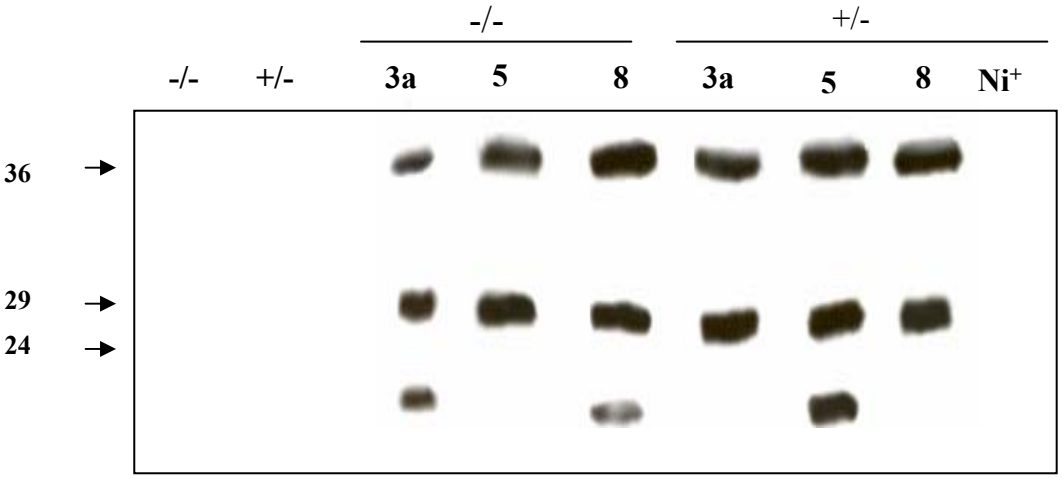

IB anti-flag 1:1000

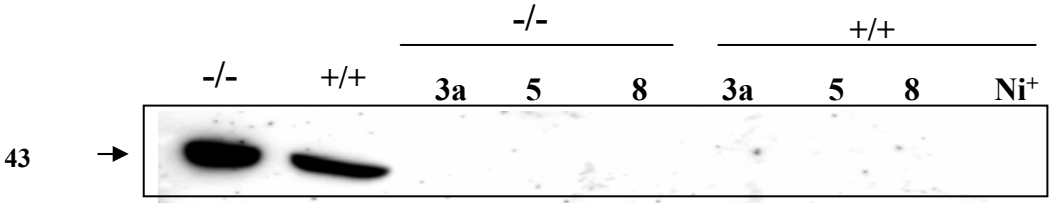

IB Anti-β-actin `1:1000

Pull-down in transgenic treated mice

MPTP-treated mice

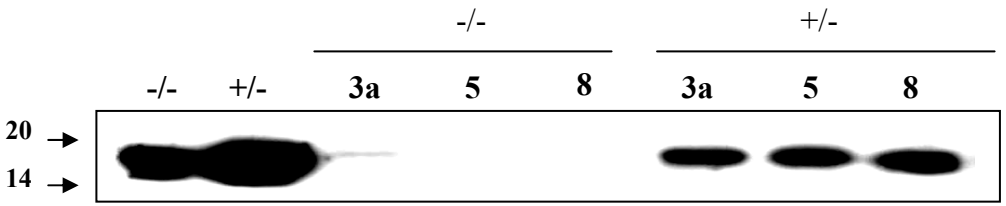

IB anti-α-syn 1:1000

Rotenona-treated mice

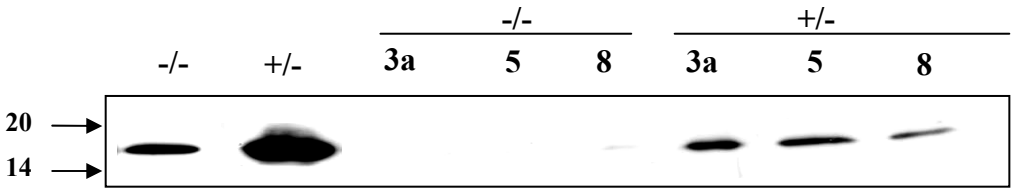

IB anti-α-syn 1:1000

Rab 5 pull-down with recombinant α-synuclein

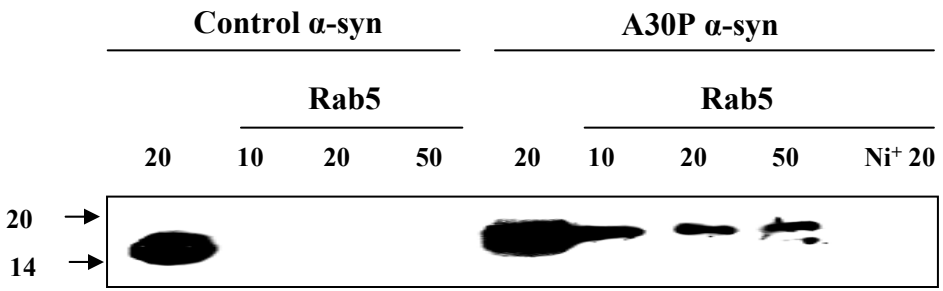

IB anti-α-syn 1:1000

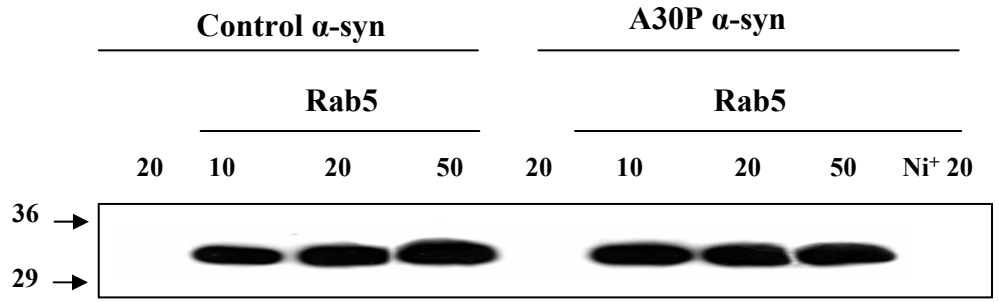

IB anti-flag 1:1000

Rab3a inmunoprecipitation in transgenic mice

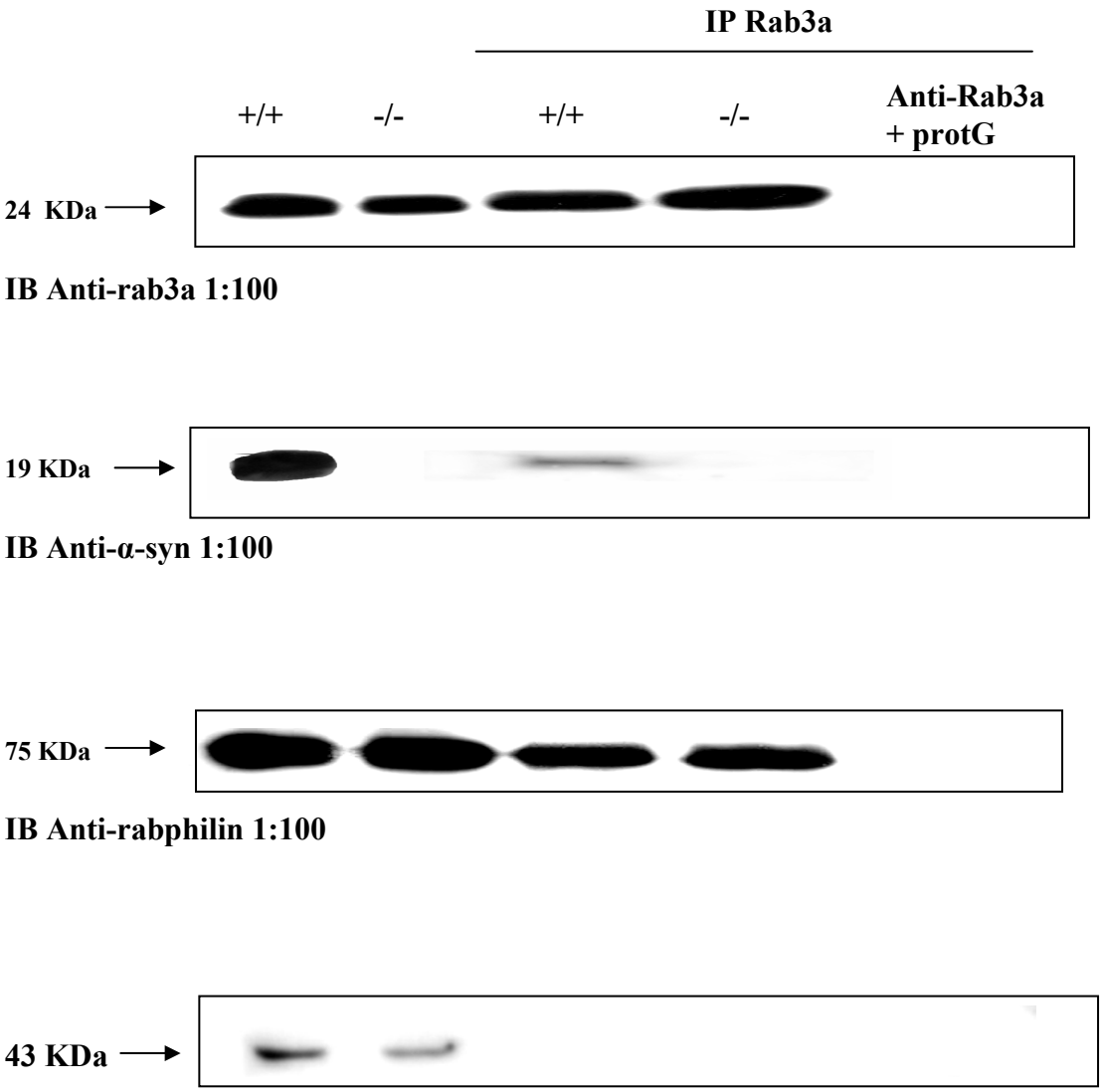

Rab3a inmunoprecipitation in human cortex

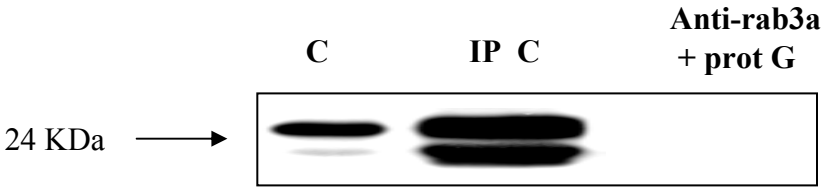

IB Anti-rab3a 1:100

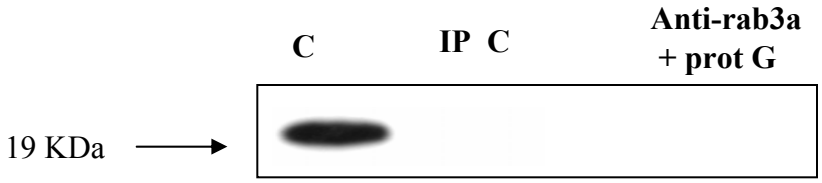

IB Anti-α-synuclein 1:100

ABNORMAL METABOTROPIC GLUTAMATE RECEPTOR EXPRESSION AND SIGNALING IN THE CEREBRAL CORTEX IN DIFFUSE LEWY BODY DISEASE IS ASSOCIATED WITH IRREGULAR α-SYNUCLEIN/PHOSPHOLIPASE C ($PLC\beta_1$) INTERACTIONS.

E. Dalfó (1), J.L. Albasanz (3), M. Martín (3) and I. Ferrer (1, 2)

(1) Instituto de Neuropatología, Servicio de Anatomía Patológica, Hospital de Bellvitge, Hospitalet de Llobregat; (2) Departamento de Biología Celular y Anatomía Patológica, Facultad de Medicina, Universidad de Barcelona, campus de Bellvitge, Hospitalet de Llobregat; (3) Departamento de Química Inorgánica, Orgánica y Bioquímica, Facultad de Químicas, Centro Regional de Investigaciones Biomédicas, Universidad de Castilla-La Mancha, Ciudad Real; SPAIN.

Corresponding author: Prof. I. Ferrer, Instituto de Neuropatología, Servicio de Anatomía Patológica, Hospital de Bellvitge, calle Feixa Llarga sn, 08907 Hospitalet de Llobregat, Spain
E- mail: 8082ifa@comb.es or iferrer@csub.scs.es

Short title: metabotropic glutamate receptors in diffuse Lewy body disease

Publicat a *Brain Pathol* 2004; 14: 388-398

Abstract

Diffuse Lewy body disease (DLBD) is a degenerative disease of the nervous system, involving the brain stem, diencephalic nuclei and cerebral cortex, associated with abnormal α-synuclein aggregation and widespread formation of Lewy bodies and Lewy neurites. DLBD presents as pure forms (DLBDp) or in association with Alzheimer's disease (AD) in the common forms (DLBDc). Several neurotransmitter abnormalities have been reported including those of the nigrostriatal and mesocorticolimbic dopaminergic system, and central noradrenergic, serotoninergic and cholinergic pathways. The present work examines metabotropic glutamate receptor (mGluR) expression and signaling in the frontal cortex of DLBDp and DLBDc cases in comparison with age-matched controls. Abnormal L-[^{3}H]glutamate specific binding to group I and II mGluRs, and abnormal $mGluR_1$ levels have been found in DLBD. This is associated with reduced expression levels of phospholipase C β1 (PLCβ1), the effector of group I mGluRs following protein G activation upon glutamate binding. Additional modification in the solubility of PLCβ1 and reduced PLCβ1 activity in pure and common DLBD further demonstrates for the first time abnormal mGluR signaling in the cerebral cortex in DLBD. In order to look for a possible link between abnormal mGluR signaling and α-synuclein accumulation in DLBD, immunoprecipitation studies have shown α-synuclein/PLCβ1 binding in controls and decreased α-synuclein/PLCβ1 binding in DLBD. This is accompanied by a shift in the distribution of α-synuclein, but not of PLCβ1, in DLBD when compared with controls. Together, these results support the concept that abnormal α-synuclein in DLBD produces functional effects on cortical glutamatergic synapses, which are associated with reduced α-synuclein/PLCβ1 interactions, and, therefore, that mGluRs are putative pharmacological targets in DLBD. Finally, these results emphasize the emergence of a functional neuropathology that has to be explored for a better understanding of the effects of abnormal protein interactions in degenerative diseases of the nervous system.

Key words: metabotropic glutamate receptors, phospholipase C, α-synuclein, diffuse Lewy body disease

Introduction

Diffuse Lewy body disease (DLBD), also called dementia with Lewy bodies, is a frequent degenerative disease of the nervous system in the elderly, characterized by the presence of abnormal α-synuclein production and deposition in the form of biochemical and structural aggregates, currently manifested as Lewy bodies in the cytoplasm of neurons and as enlarged neurites in degenerated neuronal processes that have been called Lewy neurites. Lesions are mainly encountered in selected nuclei of the medulla, serotoninergic raphe nuclei, noradrenergic locus ceruleus, substantia nigra *pars compacta,* dopaminergic mesocorticolimbic system, cholinergic nucleus basalis of Meynert and pedunculopontine nucleus, as in Parkinson's disease (PD), and in the hippocampus and entorhinal cortex, diencephalic nuclei, amygdala, gyrus cinguli and isocortex (3, 19, 28, 31, 32, 35, 38, 71). PD and DLBD are included within the spectrum of Lewy body diseases (LBDs) that have been categorized, for operational purposes, as midbrain, limbic and neocortical LBDs (21, 53, 54). The limits of these categories are not precise, and the use of new antibodies raised against oxidized α-synuclein has shown widespread α-synuclein pathology in the striatum in LBDs, higher in DLBD and lower in PD (18). Alzheimer's disease (AD) is a frequent association in DLBD. The common form of DLBD (DLBDc) is characterized by abundant senile plaques and neurofibrillary tangles, particularly in the temporal cortex, whereas the pure form of DLBD (DLBDp) comprises a subgroup of patients in whom the AD pathology is minimal (27, 43, 44). Although this association has produced much controversy, operational criteria for AD changes in DLBD are the same as those applied in conventional AD regarding βA4-amyloid burden (stages A-C) and neurofibrillary degeneration (I, II: entorhinal, III-IV: limbic and V, VI: isocortical stages) (5).

The main clinical manifestations of DLBD are parkinsonism and dementia, characterized by cognitive decline, recurrent visual hallucinations, and fluctuating cognitive state and level of consciousness. Cognitive decline includes impairment of memory, language, visuospatial ability, attention, learning visuoconstructive ability and psychomotor speed. Repeated falls, depression, rapid eye movement sleep behavior disorder, and neuroleptic sensitivity are additional clinical features in DLBD (31, 53, 54).

Several studies have shown a correlation between Lewy bodies in the cerebral cortex and Lewy neurites in amygdala with cognitive impairment (10, 30, 46, 52, 67). Cortical synaptic loss, as suggested by decreased expression of synaptophysin in the frontal cortex, probably contributes to cognitive impairment in DLBD as well (26). Yet clinical manifestations, and particularly cognitive impairment in parkinsonism, are dependent on much more sophisticated biochemical shifts (34). For example, patients with hallucinations tend to have marked cortical cholinergic deficits and relatively preserved serotoninergic systems (58, 59, 60). Moreover, AD changes in DLBDc further complicate the scenario of cognitive decline.

G-protein-coupled receptors (GPCRs) comprise the largest superfamily of proteins in the body with thousands of putative ligands including biogenic amines, peptides, glycoproteins, lipids, nucleotides and ions (24, 42). GPCRs are composed of seven sequences that span the plasma membrane in a counter-clockwise manner forming a recognition and connection unit that has the ability to interact with a G-protein. The activated receptor induces a conformational change in the associated G protein α-subunit leading to release of GDP followed by binding of GTP, which dissociates from the receptor and modulates several signaling pathways (48). These include activation or inhibition of adenylyl cyclases and activation of phospholipases, and regulation of potassium and calcium channels (24). One of the major subfamilies of GPCRs is related to the metabotropic neurotransmitter receptors. This family includes the metabotropic glutamate and GABA receptors, calcium receptors, vomeronasal pheromone receptors and taste receptors.

Metabotropic glutamate receptors (mGluRs) are classified as group I, II and III (12, 55, 57). Receptors of group I, which includes $mGluR_1$ and $mGluR_5$, are coupled with a $G_{q/11}$ protein and stimulate phospholipase $C\beta_1$ ($PLC\beta_1$) following protein G activation upon glutamate binding. Receptors of groups II and III inhibit adenylyl ciclase and activate G-protein coupled potassium channels (GIRKs). $PLC\beta_1$ activation stimulates phosphatidylinositol (PI) turnover, leading to phosphatidylinositol-4,5-biphosphate (PIP_2) hydrolysis and resulting in the generation of two intracellular messengers, inositol-1,4,5-triphosphate (IP_3) and diacylglycerol (DAG), which in turn promote the release of intracellular Ca^{2+} stores and the activation of protein kinase C (12, 25, 62, 65, 66).

Interestingly, group I and group III mGluRs modulate synaptic transmission in the striatopallidal complex (69, 73), and activation of group II mGluRs inhibits synaptic excitation of the substantia nigra *pars reticulata* (6). Blockade of group I mGluRs inhibits akinetic deficits in a rat model of parkinsonism (7, 56). Moreover, several lines of evidence implicate mGluRs as putative pharmacological targets in controlling motor deficits in PD (20, 63). However, practically nothing is known about mGluRs in the cerebral cortex in DLBD.

Synucleins have emerged as a novel class of substrates for G protein-coupled receptor kinases (64). Synucleins interact with phospholipase D2 (11, 36), and phosphorylation of α-synuclein at Ser^{129} inhibits the interaction of α-synuclein with phospholipids or phospholipase D2 (64). Synuclein interaction with phospholipase D isozymes inhibits phospholipase activation in certain paradigms (1). These data offer exciting insights based on the hypothesis that abnormal α-synuclein in LBDs may result in abnormal interactions with crucial proteins of the metabotropic receptors signaling pathways, thus leading to impaired neurotransmitter function.

In line with this rationale, the present work is focused on the study of mGluRs in the cerebral cortex in DLBD pure and common forms, with special attention to L-[^{3}H] glutamate binding and modifications in the glutamate binding to group I, group II and group III receptors, total protein expression levels of $mGluR_1$ and $PLC\beta_1$, $PLC\beta_1$ activity, and $PLC\beta_1$ solubility and interactions with α-synuclein in control and DLBD brains. Results of the present study show abnormal α-synuclein/$PLC\beta_1$ interactions associated with impaired mGluR function in the cerebral cortex in DLBD.

Material and methods

Tissue samples

Brain samples were obtained from the Institute of Neuropathology Brain Bank following the guidelines of the local ethics committee. The brains of 8 patients with DLBD pure form, 12 patients with DLBD common form and 5 age-matched controls were obtained from 3 to 13 h after death and were immediately prepared for morphological and biochemical studies. A summary of the main clinical characteristics is presented in Table I. At autopsy, half of each brain was fixed in formalin, while the other half was cut in coronal sections 1 cm thick, frozen on dry ice and stored at -80ºC until use. In addition, samples 2 mm thick of the cerebral isocortex, cingulum, hippocampus and entorhinal cortex, and brain stem were fixed with 4% paraformaldehyde for 24 h, cryoprotected with 30% saccharose, frozen on dry ice and stored at -80ºC until use. For diagnostic morphological studies, the brains were fixed by immersion in 10% buffered formalin for 2 or 3 weeks. The neuropathological study was carried out on de-waxed 4-µm-thick paraffin sections of the frontal (area 8), primary motor, primary sensory, parietal, temporal superior, temporal inferior, anterior cingulated, anterior insular, and primary and associative visual cortices; entorhinal cortex and hippocampus; caudate, putamen and pallidum; medial and posterior thalamus; subthalamus; Meynert nucleus; amygdala; midbrain (two levels), pons and medulla oblongata; and cerebellar cortex and dentate nucleus. The sections were stained with haematoxylin and eosin, luxol fast blue-Klüver Barrera, and, for immunohistochemistry to glial fibrillary acidic protein, CD68 and *Licopericum esculentum* lectin for microglia, βA4 amyloid, *tau*, αB-crystallin, α-synuclein and ubiquitin. Validated neuropathological criteria for the diagnosis of DLBDp and DLBDc are detailed elsewhere (21, 53, 54).

Plasma membranes isolation

Plasma membranes from brain samples were isolated as described by Kessler et al. (39) with some modifications. Samples were homogenized in 20 volumes of isolation buffer (50 mM Tris-HCl, pH 7.4 containing 10 mM $MgCl_2$ and protease inhibitors) in Dounce homogenizer (10xA, 10xB). After homogenization, brain preparations were centrifuged for 5 min at 1,000 xg in a Beckman JA 21 centrifuge. Supernatant was centrifuged for 20 min at 27,000 xg and the pellet was finally resuspended in isolation buffer. Protein concentration was measured by the method of Lowry, using bovine serum albumin (BSA) as a standard.

Metabotropic glutamate receptor binding to plasma membranes

L-[^{3}H]Glutamate (48.1 Ci/mmol) was purchased from PerkinElmer (Madrid). L-glutamic and α-amino-3-hydroxy-5-methyl-isoxazole-4 propionic (AMPA) acids were obtained from Tocris (London). N-methyl-D-aspartic acid (NMDA), Kainate and DL-threo-β-hydroxyaspartic acid (TBHA) were from Sigma (Madrid). L-[^{3}H]Glutamate binding assays to brain plasma membranes were performed as described previously (2, 50). Briefly, to determine mGluR binding, 50 µg of protein was incubated for 60 min at 25ºC in the presence of 100 µM AMPA, 100 µM kainate and 100 µM NMDA, in order to block ionotropic glutamate receptor binding, and different L-[^{3}H]Glutamate concentrations (50 nM - 1960 nM) with 10 mM potassium phosphate pH 7.4. Non-specific binding was obtained in the presence of unlabeled L-glutamate. All assays were performed in the presence of 1 mM DL-threo-β-hydroxyaspartic acid (THBA), a L-glutamate uptake inhibitor (41).

Immunodetection of $mGluR_1$ and the phospholipase C β_1 isoform

One hundred micrograms of protein were subjected to 7.5 % polyacrilamide gel electrophoresis in the presence of SDS. Western blotting was performed as described earlier (49). Immunodetection was carried out by incubating the nitrocellulose membranes with specific rabbit polyclonal antibody to $mGlu_1$ at a dilution of 1:1,000

and isoenzyme-specific monoclonal antibody anti-PLCβ_1 at a dilution of 1:400 (Upstate, Reactiva, Madrid). After washing, blots were incubated with horseradish peroxidase-coupled goat anti-rabbit or anti-mouse IgG, respectively, diluted 1:3,000. Antigen was visualized using the ECL chemiluminescence detection kit from Amersham and specific bands were quantified by densitometry in a GS-690 densitometer (BioRad, Madrid).

Phospholipase C assay

Phospholipase C activity in plasma membranes was assayed in the presence of exogenous phosphatidylinositol-4,5-bisphosphate, ([^{3}H]PIP_2, 8 Ci/mmol, PerkinElmer, Madrid) as described by Tiger et al. (72). [^{3}H]PIP_2 was dried under a N_2 stream, dissolved in 2 mM sodium deoxycholate, 50 mM Tris-HCl pH 6.5 and sonicated using an Ultrasonic Processor UP 200 S. Phospholipase C assay was carried out for 10 min at 37ºC, incubating [^{3}H]PIP_2 (17,000 dpm) with 20 µg of plasma membrane protein in 100 µl of buffer (100 mM NaCl, 1 mM sodium deoxycholate, 1 mM EGTA, 250 nM Cl_2Ca, 40 mM ClLi and 50 mM Tris-HCl pH 6.8) The incubation was terminated by adding 360 µl of chloroform/methanol/HCl (1:2:0.2 v/v) and putting the tubes on ice. After the addition of 120 µl 2M KCl and 160 µl of chloroform, the tubes were centrifuged for 5 min at 3,500xg. Upper aqueous phase (250 µl) was mixed with 3.5 ml of Optiphase-Hi-Safe® for scintillation counting.

α-synuclein solubility and aggregation

Brain samples (0.2 g) of the frontal cortex were homogenized in a glass homogenizer in 1.5 ml of ice-cold PBS$^+$ (sodium phosphate buffer, pH 7.0, plus protease inhibitors), sonicated and centrifuged at 2,650 xg at 4ºC for 10 min. The pellet was discarded and the resulting supernatant was ultracentrifuged at 100,000 xg at 4ºC for 1 h. The supernatant (S2) was kept as the PBS-soluble fraction. The resulting pellet was re-suspended in a solution of PBS, pH 7.0, containing 0.5% sodium deoxycholate, 1% Triton and 0.1% SDS, and it was ultracentrifuged at 100,000 xg at 4ºC for 1 h. The resulting supernatant (S3) was kept as the deoxycholate-soluble fraction. The corresponding pellet was re-suspended in a solution of SDS 2% in PBS and maintained at room temperature for 2 h. Immediately afterwards, the samples were centrifuged at 100,000 xg at 25ºC for 1 h, and the resulting supernatant (S4) was the SDS-soluble fraction. Equal amounts of each fraction were mixed with reducing sample buffer and processed for 10% SDS-PAGE electrophoresis and Western blot analysis. The membranes were incubated with anti-α-synuclein (Chemicon, Barcelona) at a dilution of 1:2,000 or with anti-PLCβ_1 (Santa Cruz, Quimigranel, Barcelona) at a dilution of 1:100. The protein bands were visualized by the ECL method (Amersham, Barcelona).

PLCβ_1 immunoprecipitation and immunoblot

Samples (0.2 g) of the frontal cortex (area 8) were homogenized in a glass homogenizer in 1.5 ml of ice-cold lysis buffer (PBS, 1 mM sodium orthovanadate, 1 mM sodium fluoride, 10 µg/ml aprotinin and 1 mM phenylmethylsulfonyl fluoride) and centrifuged at 2,650 xg for 10 min at 4 °C. The supernatant S1 was further centrifuged at 100,000 xg for 1 h at 4°C to generate the supernatant S2. Protein concentrations were determined using the BCA method with BSA as a standard. S2 fractions were diluted to roughly 1 µg/µl total protein with PBS before beginning the immunoprecipitation. Mouse monoclonal anti-PLCβ1 antibody (5 µg) (Upstate, Reactiva, Barcelona) was added to 1 mg of total protein from S2 fraction, and the mixture was gently rocked at 4ºC overnight. The immunocomplexes were captured by adding 100 µl (50 µl packed beads) of washed Protein G agarose bead slurry (Amersham Pharmacia, Barcelona). The reaction mixture was gently rocked at 4ºC for 2 hours and the agarose beads were collected by pulsing (5 sec in the microcentrifuge at 14,000 xg), and draining off the supernatant. The beads were washed 3 times with

ice-cold PBS and, finally, the agarose beads were re-suspended in 32.5 μl 4x Laemmli sample buffer and boiled for 5 min. The beads were collected using a microcentrifuge pulse, and 10% SDS-polyacrilamide gels were electrophoresed by using Mini-Protean II (BioRad, Madrid) and proteins were then transferred to nitrocellulose membranes (BioRad).
The blotted membranes were treated with PBS containing 3% skimmed milk for 20 minutes at room temperature with constant agitation, and then incubated with 5 μg/ml of monoclonal, rabbit polyclonal anti-PLCβ1 (Santa Cruz) at a dilution of 1:100, or with the rabbit policlonal anti-α-synuclein antibody (Chemicon) used at a dilution of 1:1000 in PBS containing 3% bovine albumin with agitation at 4ºC overnight. The protein bands were visualized using the chemiluminescence ECL method (Amersham), and the membranes were exposed to autoradiographic films (Hyperfilm, Amersham).

Cell fractionation by sucrose density gradients
Samples (0.2 g) from DLBD, pure and common forms, and control cases were homogenized in a glass homogenizer in 2 ml of ice-cold extraction buffer (5 mM Tris, 250 mM sucrose, 1 mM EGTA pH 7.4, plus protease and phosphatase inhibitors (1 mM sodium orthovanadate, 1 mM sodium fluoride, 10 μg/ml aprotinin, 1 mM phenylmethylsulfonyl fluoride), sonicated and centrifuged at 2,650 xg for 5 min at 4 °C. The supernatant was reserved and the pellet was resuspended in 1 ml of the same extraction buffer and centrifuged at 2,650 xg for 5 min at 4ºC. The pellet was discarded and the supernatant was pooled with the first supernatant. This postnuclear supernatant was layered onto a 10-ml, linear 0.4-2 M sucrose gradient buffered with 5 mM Tris, 1 mM EGTA pH 7.4 in 14 x 95-mm polyallomer tubes (Beckman Instruments, Madrid). Gradients were centrifuged at 100,000 xg for 3 h at 4°C (Beckman Instruments). Fractions of 500 μl were collected from the bottom of the tube and stored at -80°C.
Samples from the gradient fractions were subjected to 10% electrophoresis and western blotting with the following antibodies: rabbit polyclonal anti-α-synuclein (Chemicon) used at a dilution of 1:2,000, rabbit polyclonal anti-PLCβ1 (Santa Cruz) used at at a dilution of 1:500, mouse monoclonal anti-synaptosomal associated protein of 25 kDa (SNAP-25) (Chemicon) 1:1000, mouse monoclonal anti-synaptotagmin (a gift of Dr. J. Blasi, Barcelona, Spain) used at a dilution of 1:1,000, and mouse monoclonal anti-α-tubulin (Sigma) used at a dilution of 1:5,000. The protein bands were visualized by the ECL method (Amersham).

Immunohistochemistry
Paraformaldehyde-fixed, cryostat sections, 15 μm thick, were processed for α-synuclein and PLCβ_1 immunohistochemistry following the streptavidin LSAB method (Dako). After incubation with methanol and normal serum, the sections were incubated free-floating with one of the primary antibodies at 4ºC overnight. Antibodies to α-synuclein (Chemicon) were used at a dilution of 1:1,500; antibodies to PLCβ_1 (Santa Cruz) were used at a dilution of 1:100. Following incubation with the primary antibody, the sections were incubated with LASB for 1 h at room temperature. The peroxidase reaction was visualized with diaminobenzidine, NH_4NiSO_4 and H_2O_2. Control of the immunostaining included omission of the primary antibody; no signal was obtained following incubation with only the secondary antibody.

Statistical and data analysis
Data statistical analysis was performed using the Student *t*-test. Differences between mean values were considered statistically significant at $p<0.05$. The binding data were analyzed with the GraphPad Prism 3.03 program (GraphPad Software, San Diego, CA).

Results

Metabotropic glutamate receptor

L-[^{3}H]Glutamate binding assay performed in the presence of ionotropic agonists kainate, AMPA and NMDA revealed a single and saturable metabotropic binding site in plasma membranes from human brain. The total number of binding sites (B_{max}) was obtained by scatchard and non-linear regression analysis from saturation curves data. As shown in Figure 1, B_{max} value was slightly but significantly decreased (78% of control, $p<0.01$) in DLBDc. However, an increase in B_{max} value (217% of control, $p<0.001$) was found in DLBDp. In addition, K_D values were significantly decreased (68.9% of control value, $p<0.01$) and increased (147% of control value, $p<0.01$), respectively, in DLBDc and DLBDp, suggesting that metabotropic glutamate receptor affinity was significantly higher than in control in DLBDc and lower than in control in DLBDp.

To further analyze which mGluR groups were affected in DLBD, binding assays were performed to a single concentration of radioligand (500 nM) and in the presence of unlabelled 1 mM L-quisqualic acid (which is a very potent agonist of group I mGluRs), (2R,4R)-4-aminopyrrolidine-2,4-dicarboxylate ((2R,4R)-APDC, a selective agonist of group II mGluRs) or L-(+)-2-Amino-4-phosphonobutyric acid (L-AP4, a selective agonist of group III mGluRs). As shown in Figure 2, specific L-[^{3}H]Glutamate binding to mGluRs of groups I and II was reduced in DLBD cases when compared with controls, whereas no apparent binding modifications were observed for group III mGluRs in DLBD cases when compared with controls.

As $mGluR_1$ is the main and most studied receptor subtype involved in physiological processes such as learning and memory processing, we analyzed its protein level by Western blotting using a specific antibody that recognizes $mGluR_1$. Figure 3 shows that the expression level of this receptor was significantly higher (161%) in DLBDp when compared with controls. Yet $mGluR_1$ protein level in DLBDc was significantly lower (88%) than in controls. Both results agree with the percentage of variation detected in B_{max} values from DLBDp (217% of control) and DLBDc (78% of control) (Fig. 1), suggesting that B_{max} changes detected in DLBD cases by binding assays are mainly due to modifications in $mGluR_1$.

Phospholipase C activity

One of the most widely described effector systems coupled to mGluRs is the β_1 isoform of phospholipase C ($PLC\beta_1$). Therefore, we analyzed its presence in plasma membranes from DLBD and control cases by Western blotting. As shown in Figure 4, steady state level of $PLC\beta_1$ was significantly decreased in DLBD pure and common forms. This low quantity of β_1 isoform was, at least partially, responsible for the decreased PLC basal activity detected in DLBDp (416.2±41.8 pmol/mg prot·min) and DLBDc (442.3±48.9 pmol/mg prot.min) compared with controls (524.7±54.2 pmol/mg prot.min).

In order to study metabotropic glutamate receptor functionality, we determined the stimulatory effect exhibited by glutamate, GTP or both on PLC activity. As shown in Figure 5, L-glutamate stimulated PLC activity (139% of basal activity) in controls, and this effect was higher in the presence of GTP (168% of basal activity), thus confirming mGluR/PLC coupling through a G-protein. Yet PLC activity elicited by glutamate, GTP or both was significantly decreased (70-90% of control) in DLBD, indicating that mGluR/PLC pathway responsiveness to mGlu receptor agonists is decreased in DLBD cases, in spite of the detected increase in B_{max} value in DLDBp.

α-synuclein and PLCβ$_1$ solubility and aggregates

α-synuclein (20 kDa) was recovered in the PBS-soluble (cyt) and in the deoxycholate-soluble fractions in control and DLBD cases, but α-synuclein-immunoreactive bands in the SDS-soluble fraction only in DLBD. In addition, several α-synuclein-immunoreactive bands of high molecular weight (36 kDa, 66 kDa and higher) in the PBS-soluble, deoxycholate-soluble and SDS-soluble fractions were recovered only in DLBD (Fig. 6).

PLCβ$_1$-specific bands of ~150 kDa were recovered in the PBS-soluble fraction (cyt) and deoxycholate-soluble fractions in control and DLBD cases, although the intensity of these bands was lower in diseased than in control cases. However, PLCβ$_1$ was increased in the SDS-soluble fraction in DLBD, and several bands of about 45 and 60 kDa appeared only in disease (Fig. 7).

PLCβ$_1$ immunoprecipitation

As shown in Figure 8, immunoprecipitation with the mouse monoclonal anti-PLCβ$_1$ antibody disclosed specific bands in control and DLBD cases following incubation with the rabbit polyclonal anti-PLCβ antibody. Incubation of the membranes with anti-α-synuclein showed specific bands (20 kDa) in control and DLBD total homogenates, and in control PLCβ$_1$-immunoprecipitate samples. No α-synuclein was recovered in PLCβ$_1$-immunoprecipitates from DLBD cases. These results were not dependent on the relative amount of total protein between DLBD and control cases, as seen in IP lanes blotted for PLCβ$_1$. Similar results were obtained in DLBDp and DLBDc (Fig. 8 A and B).

Cell fractionation by sucrose density gradients

Cell fractionation revealed that the distributions of tubulin, synaptotagmin (not shown) and SNAP-25 (Fig. 9 upper panel) were similar in DLBD and control cases. However, the subfractionation distribution of α-synuclein (a band of about 20 kDa) in DLBD cases differed from controls, as the amount of α-synuclein was reduced in the so-called synaptic fractions (Fig. 9 middle panel). The distribution of PLCβ1 (150 kDa) was similar in DLBD cases and controls (Fig. 9 inner panel). Similar results were obtained in DLBDp and DLBDc cases.

PLCβ$_1$ immunohistochemistry

In order to rule out possible accumulation of PLCβ$_1$ in Lewy bodies and Lewy neurites, immunohistochemistry was used to show localization of PLCβ$_1$ immunoreactivity in the cell bodies of cortical neurons in control and DLBD cases. However, Lewy bodies and Lewy neurites were not stained with anti-PLCβ1 antibodies, as revealed in consecutive sections stained with anti-α-synuclein (Fig. 10).

Discussion

Several studies have dealt with neurotransmitter deficits in PD and DLBD, most of these correlating with neuronal loss of the corresponding vulnerable nuclei to LBDs. Less is known about possible abnormalities of neurotransmitter receptors that may sustain impaired cognitive functions. Yet recent studies have shown reduced dopaminergic (70) and acetylcholine nicotinic (51, 61) receptors in the cerebral cortex in DLBD, thus probably accounting, in part, for the cognitive impairment in these patients.
The present work has shown abnormal L-[^{3}H]glutamate specific binding to group I and II mGluRs, and abnormal $mGluR_1$ levels in the cerebral cortex in DLBD. In addition to abnormal glutamate binding, reduced $PLC\beta_1$ levels and reduced $PLC\beta_1$ activity have been found in DLBD, pure and common forms. These findings demonstrate abnormal mGluR receptor signaling in the cerebral cortex in DLBD.
Reduced [^{3}H]glutamate metabotropic binding in the subiculum and CA1 region of the hippocampus (16), and decreased $PLC\beta_1$ and PKC levels and activity (13, 74), have been reported in AD. It can be suggested that associated AD changes may explain mGluR deficits in DLBDc. However, the present findings clearly indicate abnormal mGluR patterns in DLBDp, thus demonstrating primary mGluR impairment in DLBD. Interestingly, the expression levels of $mGluR_1$ are higher in DLBDp and lower in DLBDc when compared with control values. Whether this is a reflection of up-regulation or low turnover of $mGluR_1$ receptors in DLBDp is not known, but this aspect further emphasizes peculiar abnormalities in DLBD not associated with AD changes.

It is tempting to speculate that α-synuclein plays a role in the abnormal mGlu receptor signaling in DLBD. Previous studies have shown insoluble α-synuclein and formation of biochemical aggregates in DLBD cases (8, 33). Multiple α-synuclein bands of variable solubility have also been observed in the present study. Furthermore, fractionation studies have shown a discrete shift consistent with modifications in the motility of DLBD α-synuclein in sucrose gradients. Western blots of formic acid-treated Lewy bodies isolated from DLBD cortex show partially truncated forms of α-synuclein and several bands of variable molecular weight consistent with α-synuclein-immunoreactive aggregates (3, 33). In addition, α-synuclein is nitrated (17, 23), and residue Ser^{129} of α-synuclein is selectively and extensively phosphorylated in PD and DLBD (22, 33). Moreover, phosphorylation of α-synuclein at Ser^{129} promotes fibril formation (22). Finally, altered conformation of α-synuclein and direct intermolecular interaction between the N-terminus of α-synuclein and ubiquitin occurs in Lewy bodies when compared with the neuropil (68). Yet immunohistochemical studies have ruled out $PLC\beta_1$ immunoreactivity in Lewy bodies and Lewy neurites.

Previous studies have shown that synaptic vesicle trafficking is probably impaired in DLBD as a result of abnormal interactions of α-synuclein with members of the rab protein family, including rab3a and its associated protein rabphilin, in the cerebral cortex of patients with DLBD (14). Similar abnormal α-synuclein/rab interactions occur in the brains of transgenic mice expressing high levels of mutant A30P α-synuclein (15).

The present results have shown multiple $PLC\beta_1$ bands from 45 kDa to about 150 kDa kDa in the deoxycholate-soluble and SDS-soluble fractions in DLBD, thus indicating the presence of probable truncated forms of $PLC\beta_1$, abnormal $PLC\beta_1$ solubility in PBS, deoxycholate and urea, and abnormal solubility of $PLC\beta_1$ in sucrose gradients in DLBD. Previous studies have demonstrated α-synuclein interaction with phospholipase D isozymes and α-synuclein inhibition of pervanadate-induced phospholipase D activation in embryonic kidney cell lines (1). The present immunoprecipitation studies have shown α-synuclein interaction with $PLC\beta_1$ in cortical brain homogenates from

control subjects, and decreased PLCβ_1/α-synuclein binding in DLBD. Interestingly, phosphorylation of α-synuclein at Ser129, as occurs in LBDs, also inhibits the interaction of α-synuclein with phospholipase D (64). Together, these findings indicate that expression and activity of PLCβ_1, a crucial protein in the signaling pathway of group I mGluRs, is abnormal in DLBD, and that this abnormal activity is associated with an anomalous interaction of this protein with α-synuclein resulting in decreased PLCβ_1/α-synuclein binding in DLBD.

mGluRs modulate excitability and synaptic transmission. Group I mGluRs increase neural excitability through inhibition of potassium conductances and activation of non-selective cation currents. Synaptic transmission is also regulated presynaptically and postsynaptically by mGluRs. Presynaptically, mGluRs depress glutamate release from presynaptic nerve terminals through calcium channel inhibition, and this capacity is ubiquitous. In addition, postsynaptic modulation of mGluRs is much more specific. For example, agonists of group I mGluRs potentiate N-methyl-D-aspartate acid (NMDA) receptor currents, but not α-amino-3-hydroxy-5-methyl-4-isoxalonepropionate acid (AMPA) receptor currents, in the hippocampus. Considering these properties, it is conceivable that major cortical functional deficits may be attributed to abnormal mGluR processing and PLCβ_1 signaling. In addition, observations in PLCβ_1-null mice have shown that PLCβ_1 is involved in the development and control of brain inhibitory pathways (4, 40, 65). Finally, group I mGluRs accelerate the processing of amyloid precursor protein (APP) into non-amyloidogenic APPs (29, 37, 45, 47). Therefore, reduced group I mGluR activity may facilitate amyloidogenic APP processing, thus contributing to the formation and deposition of βA4-amyloid, in DLBD. Alternatively, increased amyloid deposition may result in reduced mGluR expression and activity. However, observations in Tg2576 mice expressing human APP with the Swedish?? double mutation K670N-M671L have shown no significant alteration in group I and II metabotropic glutamate receptors (9).

Blockade of group I mGluRs inhibits akinetic deficits in a rat model of parkinsonism (5, 56), and activation of group II mGluRs inhibits synaptic excitation of the substantia nigra *pars reticulata* (6). These and other activities have served to implicate mGluRs as putative pharmacological targets in controlling motor deficits in PD (20, 63). The present findings further support a rationale for considering mGluRs as additional possible pharmacological targets in the control of cognitive deficits in DLBD.

References

1. Ahn BH, Rhim H, Kim SY, Sung YM, Lee MY, Choi JY, Wolozin B, Chang JS, Lee YH, Kwon TK, Chung KC, Yoon SH, Hahn SJ, Kim MS, Jo YH, Min DS (2002) α-synuclein interacts with phospholipase D isozymes and inhibits pervadanate-induced phospholipase D activation in human embryonic kidney-293 cells. *J Biol Chem* 277: 12334-12342.
2. Albasanz JL, Leon D, Ruiz MA, Fernandez M, Martin M (2002) Adenosine A1 receptor agonist treatment up-regulates rat brain metabotropic glutamate receptors. *Biochim Biophys Acta* 1593: 69-75.
3. Baba M, Nakajo S, Tu PH, Tomita T, Nakaya K, Lee VMY, Trojanowski JQ, Iwatsubo T (1998) Aggregation of α-synuclein in Lewy bodies of sporadic Parkinson's disease and dementia with Lewy bodies. *Am J Path*ol 152: 879-884.
4. Böhm D, Schwegler H, Kotthaus L, Nayernia K, Rickmann M, Köhler M, Rosenbusch J, Engel W, Flügge G, Burfeind P (2002) Disruption of PLCβ1-mediated signal transduction in mutant mice causes age-dependent hippocampal mossy fiber sprouting and neurodegeneration. *Mol Cell Neurosci* 21: 584-601.
5. Braak H, Braak E (1999) Temporal sequence of Alzheimer's disease-related pathology. In: *Cerebral cortex vol 14: Neurodegenerative and age-related changes in structure and function of cerebral cortex*. Peters A, Morrison JH (eds.), pp 475-512, Kluwer Academic/Plenum Press: New York, Boston, Dordrecht, London, Moscow.
6. Bradley SR, Marino MJ, Wittmann M, Rouse ST, Awad H, Levey AI, Conn.PJ (2000) Activation of group II metabotropic glutamate receptors inhibit synaptic excitation of the substantia nigra pars reticulata. *J Neurosci* 20: 3085-3094.
7. Breysse N, Baunez C, Spooren W, Gasparini F, Amalric M (2002) Chronic but not acute treatment with a metabotropic glutamate 5 receptor antagonist reverses the akinetic deficits in a rat model of parkinsonism. *J Neurosci* 22: 5669-5678.
8. Campbell BC, Li QX, Culvenor JG, Jakala P, Cappai R, Beyreuther K, Masters CL, McLean CA (2000) Accumulation of insoluble α-synuclein in dementia with Lewy bodies. *Neurobiol Dis* 7: 192-200.
9. Cha JHJ, Farrell LA, Ahmed SF, Frey A, Hsiao-Ashe KK, Young AB, Penney JB, Locascio JJ, Hyman BT, Irizarry MC (2001) Glutamate receptor dysregulation in the hippocampus of transgenic mice carrying mutated human amyloid precursor protein. *Neurobiol Dis* 8: 90-102.
10. Churchyard A, Lees AJ (1997) The relationship between dementia and direct involvement of the hippocampus and amygdala in Parkinson's disease. *Neurology* 49: 1570-1576.
11. Colley WC, Sung TC, Roll R, Jenco J, Hammond SM, Altshuller Y, Bar-Sagi D, Morris AJ, Frohman MA (1997) Phospholipase D2, a distinct phospholipase D isoform with novel regulatory properties that provokes cytoskeletal reorganization. *Curr Biol* 7: 191-201.
12. Conn P, Pin JP (1997) Pharmacology and functions of metabotropic glutamate receptors. Ann Rev Pharmacol Toxicol 37: 205-237.
13. Cowburn RF, O'Neill C, Bonkale WL, Ohm TG, Fatbom J (2001) Receptor-G-protein signalling in Alzheimer's disease. *Biochem Soc Symp* 67: 163-175.
14. Dalfó E, Barrachina M, Rosa JL, Ambrosio S, Ferrer I (2004) Abnormal α-synuclein interactions with rab3a and rabphilin in diffuse Lewy body disease. *Neurobiol Dis* (in press).
15. Dalfó E, Gómez-Isla T, Rosa JL, Nieto Bodelón M, Cuadrado Tejedor M, Barrachina M, Ambrosio S, Ferrer I (2004) Abnormal synuclein interactions with Rab proteins in synuclein A30P transgenic mice. *J Neuropatyhol Exp Neurol* (in press).
16. Dewar D, Chalmers DT, Graham DI, McCulloch J (1991) Glutamate metabotropic and AMPA binding sites are reduced in Alzheimer's disease: An autoradiographic study of the hippocampus. *Brain Res* 553: 58-64.

17. Duda JE, Giasson BI, Chen Q, Gur TL, Hurtig HI, Stern MB, Gollomp SM, Ischiropoulos H, Lee VMY, Trojanowski JQ (2000) Widespread nitration of pathological inclusions in neurodegenerative synucleinopathies. *Am J Pathol* 157: 1439-1445.
18. Duda JE, Giasson BI, Mabon ME, Lee VMY, Trojanowski JQ (2002) Novel antibodies to synuclein show abundant striatal pathology in Lewy body diseases. *Ann Neurol* 52: 205-210.
19. Duda JE, Lee VMY, Trojanowski JQ (2000) Neuropathology of synuclein aggregates: new insights into mechanisms of neurodegenerative diseases. *J Neurosci Res* 61: 121-127.
20. Feeley Kearney JA, Albin RL (2003) mGluRs: a target for pharmacotherapy in Parkinson's disease. *Exp Neurol 184*, suppl 1:S30-36.
21. Ferrer I (2002) The neuropathological spectrum of Lewy body disorders. In: *Neurodegenerative disorders associated with α-synuclein pathology*, Tolosa E, Schulz JB, McKeith IG, Ferrer I (eds.), pp. 83-98, Ars Medica: Barcelona.
22. Fujiwara H, Hasegawa M, Dohmae N, Kawashima A, Masliah E, Goldberg MS, Shen J, Takio K, Iwatsubo T (2002) α-synuclein is phosphorylated in synucleinopathy lesions. *Nature Cell Biol* 4: 160-164.
23. Giasson BI, Duda JE, Murray IV, Chen Q, Souza JM, Hurrig HI, Ischiropoulos H, Trojanowski IQ, Lee VM (2000) Oxidative damage linked to neurodegeneration by selective α-synuclein nitration in synucleinopathy lesions. *Science* 290: 985-989.
24. Hamm HE (1998) The many faces of G protein signaling. *J Biol Chem* 273: 669-672.
25. Hammond C (2003) *Cellular and Molecular Neurobiology*. Chapter 14: The metabotropic glutamate receptors, pp. 314-326, Academic Press: Amsterdam, Boston, Heidelberg, London, New York, Oxford, Paris, San Diego, San Francisco, Singapore, Sydney, Tokyo.
26. Hansen LA, Daniel SE, Wilcock GK, Love S (1998) Frontal cortical synaptophysin in Lewy body diseases: relation to Alzheimer's disease and dementia. *J Neurol Neurosurg Psychiatr* 64: 653-656.
27. Hansen LA, Samuel W (1997) Criteria for Alzheimer's disease and the nosology of dementia with Lewy bodies. *Neurology* 48: 126-132.
28. Hashimoto M, Masliah E (1999) Alpha-synuclein in Lewy body disease and Alzheimer's disease. *Brain Pathol* 9: 707-720.
29. Hölscher C (1998) Possible causes of Alzheimer's disease: amyloid fragments, free radicals, and calcium homeostasis. *Neurobiol Dis* 5:129-141.
30. Hurtig HI, Trojanowski JQ, Galvin J, Ewbank D, Schmidt ML, Lee VM, Clark CM, Gloser G, Stern MB, Gollomp SM, Arnold SE (2000) α-synuclein cortical Lewy bodies correlate with dementia in Parkinson's disease. *Neurology* 54: 1916-1921.
31. Ince PG, McKeith IG (2003) Dementia with Lewy bodies. In: *Neurodegeneration: The molecular pathology of dementia and movement disorders*, Dickson D (eds.), pp188-197, ISN Neuropath Press: Basel.
32. Ince PG, Perry EK, Morris CM (1998) Dementia with Lewy bodies. A distinct non-Alzheimer dementia syndrome. *Brain Pathol* 8: 299-324.
33. Iwatsubo T (2003) Aggregation of α-synuclein in the pathogenesis of Parkinson's disease. *J Neurol* 250 suppl 3: 11-14.
34. Jellinger K (1997) Morphological substrates of dementia in parkinsonism. A critical update. *J Neural Transm* 52: Suppl. 57-82.
35. Jellinger K, Mizuno Y (2003) Parkinson's disease. In: *Neurodegeneration: The molecular pathology of dementia and movement disorders*, Dickson D (eds.), pp 159-187, ISN Neuropath Press: Basel.
36. Jenko JM, Rawlingson A, Daniels B, Morris AJ (1998) Regulation of phospholipase D2: selective inhibition of phospholipase D isoenzymes by alpha- and beta-synucleins. *Biochemistry* 37: 4901-4909.

37. Jolly-Tornetta C, Gao ZY, Lee V, Wolf BA (1998) Regulation of amyloid precursor protein secretion by glutamate receptors in human Ntera 2 neurons. *J Biol Chem* 273: 14015-14021.
38. Kahle P, Haass C, Kretszchmar HA, Neumann M (2002) Sructure/function of α-synuclein in health and disease: rational development of animal models for Parkinson's disease and related disorders. *J Neurochem* 82: 449-457.
39. Kessler M, Terramani T, Lynch G, Baudry M (1989) A glycine site associated with N-methyl-D-aspartic acid receptors: characterization and identification of a new class of antagonist. *J Neurochem* 52: 1319-28.
40. Kim D, Jun KS, Lee SB, Kang NG, Min DS, Kim YH, Ryu SH, Suh PG, Shin SH (1997) Phospholipase C isozymes selectively couple to specific neurotransmitter receptors. *Nature* 389: 290-293.
41. Kimelberg HK, Pang S, Treble DH (1989) Excitatory amino acid-stimulated uptake of $^{22}Na^{+}$ in primary astrocyte cultures. *J Neurosci* 9: 1141-9.
42. Kolakowski LF (1994) GCRDb: a G-protein-coupled receptor database. *Receptor Channels* 2: 1-7.
43. Kosaka K (1993) Dementia and neuropathology in Lewy body disease. *Adv Neurol* 60: 456-463.
44. Kosaka K, Iseki E (1996) Diffuse Lewy body disease within the spectrum of Lewy body disease. In: *Dementia with Lewy bodies*, Perry RH, McKeith IG, Perry EK (eds.), pp. 238-247, Cambridge University Press: Cambridge.
45. Lee RK, Jimenez J, Cox AJ, Wurtman RJ (1996) Metabotropic glutamate receptors regulate APP processing in hippocampal neurons and cortical astrocytes derived from fetal rats. *Ann NY Acad Sci* 777: 338-343.
46. Lennox G, Lowe J, Landon M, Byrne EJ, Mayer RJ, Godwin-Austen RB (1989) Diffuse Lewy body disease: correlative neuropathology using anti-ubiquitin immunohistochemistry. *J Neurol Neurosurg Psychiatr* 52: 1236-1247.
47. Louzada PR, Paula Lima AC, de Mello FG, Ferreira ST (2001) Dual role of glutamatergic neurotransmission on amyloid beta (1-42) aggregation and neurotoxicity in embryonic avian retina. Neurosci Lett 301: 59-63.
48. Marinissen MJ, Gutkind JS (2001) G-protein-coupled receptors and signaling networks: emerging paradigms. *Trends Pharmacol Sci* 22: 368-376.
49. Martin M, Albasanz JL, Fernandez M, Ros M (1998) Cross-talk between beta-adrenergic and metabotropic glutamate receptors in rat C6 glioma cells. *Biochem Biophys Acta* 1393: 186-92.
50. Martin M, Sanz JM, Cubero A (1993) Characterization of metabotropic glutamate receptors coupled to a pertussis toxin sensitive G-protein in bovine brain coated vesicles. *FEBS Let.* 316: 191-6.
51. Martin-Ruiz C, Lawrence S, Piggott M, Kuryatov A, Lindstrom J, Gotti C, Cookson MR, Perry RH, Jaros E, Perry EK, Court JA (2002) Nicotinic receptors in the putamen of patients with dementia with Lewy bodies and Parkinson's disease: relation to changes in alpha-synuclein expression. Neurosci Lett 335:134-138.
52. Mattila PM, Rinne JO, Helenius H, Dickson DW, Roytta M (2000) synuclein-immunoreactive cortical Lewy bodies are associated with cognitive impairment in Parkinson's disease. *Acta Neuropathol* 100: 285-290.
53. McKeith IG, Ballard CG, Pery RH, Ince PG, O'Brien JT, Neill D, Lowery K, Jaros E, Barber R, Thompson P, Swann A, Fairbairn AF, Perry EK (2000) Prospective validation of consensus criteria for the diagnosis of dementia with Lewy bodies. *Neurology* 54: 1050-1058.
54. McKeith IG, Galasko D, Kosaka K, Perry EK, Dickson DW, Hansen LA, Salmon DP, Lowe J, Mirra SS, Byrne EJ, Lenox G, Quinn NP, Edwardson JA, Ince PG, Bergeron C, Burns A, Miller BL, Lovestone S, Collerton D, Jansen EN, Ballard C, de Vos RA, Wilcock GK, Jellinger KA, Perry RH (1996) Consensus guidelines for the clinical and pathologic diagnosis of dementia with Lewy bodies (DLB): report of the consortium on DLB international workshop. *Neurology* 47: 1113-1124.

55. Michaelis EK (1998) Molecular biology of glutamate receptors in the central nervous system and their role in excitoxicity, oxidative stress and aging. *Progr Neurobiol* 54: 369-415.
56. Ossowska K, Wardas J, Pietraszek M, Konieczny J, Wolfarth S (2003) The striatopallidal pathway is involved in antiparkinsonian-like effects of the blockade of group I metabotropic glutamate receptors in rats. *Neurosci Lett* 342: 21-24.
57. Ozawa S, Kamiya H, Tsuzuki K (1998) Glutamate receptors in the mammalian central nervous system. *Progr Neurobiol* 54: 518-618.
58. Perry EK, Marshall E, Kerwin J, Smith CJ, Jabeen S, Cheng AV, Perry RH (1990) Evidence of a monoaminergic-cholinergic imbalance related to visual hallucinations in Lewy body dementia. *J Neurochem* 55 1454-1456.
59. Perry EK, Marshall E, Perry RH, Irving D, Smith CJ, Blessed G, Fairbain AF (1990) Cholinergic and dopaminergic activities in senile dementia of the Lewy body type. *Alzheimer's Dis Assoc Dis* 4: 87-95.
60. Perry EK, Marshall E, Thompson P, McKeith IG, Collerton D, Fairbain AF, Ferrier IN, Irving D, Perry RH (1993) Monoaminergic activities in Lewy body dementia: relation to hallucinations and extrapyramidal features. *J Neural Transm* 6: 167-177.
61. Pimlott SL, Piggott M, Owens J, Greally E, Court JA, Jaros E, Perry RH, Perry EK, Wyper D (2004) Nicotinic acetylcholine receptor distribution in Alzheimer's disease, dementia with Lewy bodies, Parkinson's disease, and vascular dementia: in vitro binding study using 5-[(125)i]-a-85380. *Neuropsychopharmacology* 29:108-116.
62. Pin JP, Acher F (2002) The metabotropic glutamate receptors: structure, activation, mechanisms and pharmacology. *Curr Drug Target CNS Neural Disord* 1: 297-317.
63. Pisani A, Bonsi P, Centonze D, Gubellini P, Bernardi G, Calabresi P (2003) Targeting striatal cholinergic interneurons in parkinson's disease. Focus on metabotropic glutamate receptors. *Neuropharmacol* 45: 45-56.
64. Pronin AN, Morris AJ, Surgunchov A, Benovic JL (2000) Synucleins are a novel class of substrates for G protein-coupled receptor kinases. *J Biol Chem* 275: 26515-26522.
65. Rebecchi MJ, Pentyala SN (2000) Structure, function, and control of phosphoinositide-specific phospholipase C. *Physiol Rev* 80: 1291-1335.
66. Rhee SG (2001) Regulation of phosphoinositide-specific phospholipase C. *Annu Rev Biochem* 70: 281-312.
67. Samuel W, Galasko D, Masliah E, Hansen LA (1996) Neocortical Lewy body counts correlate with dementia in the Lewy body variant of Alzheimer's disease. *J Neuropathol Exp Neurol* 55: 44-52.
68. Sharma N, McLean P, Kawamata H, Irizarry MC, Hyman BT (2001) Alpha-synuclein has an altered conformation and shows a tight intermolecular interaction with uqbiquitin in Lewy bodies. *Acta Neuropathol* 102: 329-334.
69. Smith Y, Charara A, Hanson JE, Paquet M, Levey AI (2000) GABA (B) and group I metabotropic glutamate receptors in the striatopallidal complex in primates. *J Anat* 196: 555-576.
70. Sweet RA, Hamilton RL, Healy MT, Wisniewski SR, Henteleff R, Pollock BG, Lewis DA, DeKosky ST (2001) Alterations of striatal dopamine receptor binding in Alzheimer's disease are associated with Lewy body pathology and antemortem psychosis. *Arch Neurol* 58: 466-472.
71. Takeda A, Mallory M, Sundsmo M, Honer W, Hansen L, Masliah E (1998) Abnormal accumulation of NACP/alpha-synuclein in neurodegenerative diseases. *Am J Pathol* 152: 367-72.
72. Tiger G, Bjorklund PE, Cowburn RF, Garlind A, O'Neill C, Wiehager B, Fowler CJ (1990) Effect of monovalent ions upon G proteins coupling muscarinic receptors to phosphoinositide hydrolysis in the rat cerebral cortex. *Eur J Pharmacol* 188: 51-62.
73. Valenti O, Marino MJ, Wittmann M, Lis E, DiLella AG, Kinnery GG, Conn PJ (2003) Group III metabotropic glutamate receptor-mediated modulation of the striatopallidal synapse. *J Neurosci* 23: 7218-7226.

74. Young RA, Talbot K, Gao ZY, Trojanowski JQ, Wolf BA (1999) Phospholipase pathway in Alzheimer's disease brains: decreased $G_{\alpha 1}$ in dorsal prefrontal cortex. *Mol Brain Res* 66: 188-190.

Acknowledgements

This work was supported in part by FIS grants P102/0004, G03/167 and C03/06, Brain Net II contract, and grant GC03017 from the Consejería de Sanidad of JCCM. We wish to thank T. Yohannan for editorial assistance.

FIGURE LEGENDS

Fig. 1: Saturation binding curve for metabotropic glutamate receptors. Plasma membranes (50 µg protein) from control, DLBD pure form (DLBDp) and common form (DLBDc) cases were incubated with L-[^{3}H]Glutamate in a concentration range from 50 nM to 1960 nM as described in Methods. Data points are means ± SEM of five to ten experiments performed in duplicate, each using different membrane preparations. K_D and B_{max} values from Scatchard analysis of saturation curves are shown in the inset. ** p<0.01, *** p<0.001 significantly different from control.

Fig. 2: Specific L-[^{3}H]Glutamate binding to different metabotropic glutamate receptor groups. Plasma membranes (50 µg protein) from control, DLBD pure form (DLBDp) and common form (DLBDc) cases were incubated with 500 nM L-[^{3}H]Glutamate in the absence or the presence of 1 mM quisqualic acid (group I), 1 mM (2R,4R)-APDC (group II) or 1 mM L-AP4 (group III), as described in Methods. Data are means ± SEM of, at least, three experiments performed in duplicate, each using different membrane preparations. * p<0.05 significantly different from control value.

Fig. 3: Immunodetection of $mGluR_{1a}$ in plasma membranes from human cerebral cortex. Identical quantities (100 µg) of plasma membranes from control, DLBD pure form (DLBDp) and common form (DLBDc) cases were subjected to 7.5 % SDS-PAGE, electrophoretically transferred to nitrocellulose and tested with the specific antibody against $mGluR_{1a}$ protein, as described in Methods. Data are means ± SEM of the densitometric quantification of four independent experiments performed with different membrane preparations. ** p<0.01 significantly different from control. Inset shows bands of a representative experiment.

Fig. 4: Immunodetection of PLC β_1 isoform in plasma membranes from human cerebral cortex. Identical quantities (100 µg) of plasma membranes from control, DLBD pure form (DLBDp) and common form (DLBDc) cases were subjected to 7.5 % SDS-PAGE, electrophoretically transferred to nitrocellulose and tested with the isoform-specific monoclonal antibody against PLC β_1 isoform, as described in Methods. Figure shows densitometric quantification (means ± SEM) of four independent experiments performed with different membrane preparations. * p<0.05, ** p<0.01 significantly different from control. Inset shows bands of a representative experiment.

Fig. 5: Metabotropic glutamate receptors/phospholipase C activity coupling. Twenty micrograms of plasma membranes from control, DLBD pure form (DLBDp) and common form (DLBDc) cases were incubated with [^{3}H]PtdInsP_2 in the presence of 100 µM GTP (GTP), 1 mM L-Glutamate (Glu) or both (Glu+GTP) and phospholipase C (PLC) activity determined, as described in Methods. Data are means ± SEM of four to nine experiments performed in duplicate. * p<0.05, ** p<0.01, *** p<0.001 significantly different from control. All data were significantly different (at least p<0.01) from the respective basal value in control and DLBD membranes. Basal PLC activities were 524.7±54.2, 416.2±41.8 and 442.3±48.9 pmol/mg prot·min in control, DLBDp and DLBDc cases, respectively.

Fig. 6: α-synuclein solubility. Solubility and aggregation α-synuclein examined in brain homogenates of control (C) and DLBD cases blotted for α-synuclein. A specific band of 20 kDa is recovered in the PBS-soluble (Cyt) and deoxycholate-soluble (Dxc) fractions in C and DLBD cases, and in the SDS-soluble fraction in DLBD. In addition, bands of high molecular weight of 34 kDa, 66 kDa and higher are detected in the Cyt-, Dxc- and SDS-soluble fractions only in DLBD.

Fig 7: PLCβ_1 solublity. Solubility and aggregation of PLCβ_1 examined in brain homogenates of control (C) and DLBD cases, blotted for PLCβ_1 and processed in parallel. PLCβ_1 specific bands of about 150 kDa were recovered in the PBS-soluble (Cyt) and deoxycholate-soluble (Dxc) fractions in C and DLBD cases, although the intensity of the bands was higher in the control than the diseased brain. In addition, a strong PLCβ_1 band is found in SDS-soluble fraction in DLBD. Finally, several bands of variable molecular weight (45 kDa, 60 kDa and higher) are found in the Cyt-, Dxc- and SDS-soluble fractions in DLBD.

Fig. 8: Immunoprecipitation. PLCβ_1 immunoprecipitation in brain homogenates of control (C) and DLBD cases blotted for PLCβ_1 and α-synuclein. PLCβ_1-immunoreactive bands are observed in total homogenates (TH) of C and DLBD cases, but only in the IP lane corresponding to the control and not in the lane corresponding to the diseased cases. No signal is found in the lane incubated only with protein G plus antibody (B+M). Similar results are seen in DLBD pure forms (DLBDp) (A) and common forms (DLBDc) (B).

Fig. 9: Sucrose gradients. Cell fractionation by sucrose density gradients of frontal homogenates in control and DLBD cases processed in parallel and blotted for SNAP-25, α-synuclein and PLCβ_1. Two main pools were recovered in the process. The synaptic pool was represented by SNAP-25 (25 kDa). While in control cases α-synuclein (20 kDa) was distributed in both pools, α-synuclein in the synaptic pool was dramatically decreased in DLBD. Yet PLCβ_1 (150 kDa) was detected in the cytosolic and synaptic pools equally in control and DLBD cases.

Fig. 10: α-synuclein and PLCβ1 immunohistochemistry. Immunohistochemical sections processed for α-synuclein (A) and PLCβ1 (B) in the cingulate cortex of a patient with DLBD pure form showing lack of PLCβ_1 immunostaining of Lewy bodies and Lewy neurites. Cryostat sections processed free-floating, without counterstaining, bar = 25 µm.

TABLE I

Case number	Gender	Age	P-m delay	Diagnosis
1	M	60	8	DLBDp
2	M	68	12	DLBDp
3	M	85	7	DLBDp
4	M	81	16	DLBDp
5	F	72	3	DLBDp
6	F	70	8	DLBDp
7	F	77	5	DLBDp
8	F	70	8	DLBDp
9	M	78	6	DLBDc+AD I
10	F	81	6	DLBDc+AD I
11	F	71	5	DLBDc+AD II
12	M	76	9	DLBDc+AD II
13	F	78	7	DLBDc+AD III
14	M	84	5	DLBDc+AD III
15	F	76	8	DLBDc+AD V
16	F	84	4	DLBDc+AD V
17	F	78	13	DLBDc+AD V
18	F	84	1	DLBDc+AD V
19	F	91	5	DLBDc+AD VI
20	F	80	4	DLBDc+AD VI
21	M	82	11	C
22	H	63	7	C
23	M	46	10	C
24	M	80	11	C
25	H	79	7	C

Summary of the main clinical and neuropathological data in the present series. M: male; F: female; DLBDp, DLBDc: Diffuse Lewy body disease pure and common forms, respectively; AD: Alzheimer's disease stage I-VI of Braak and Braak; P-m delay: post-mortem delay between death and tissue processing, in hours.

Fig. 1

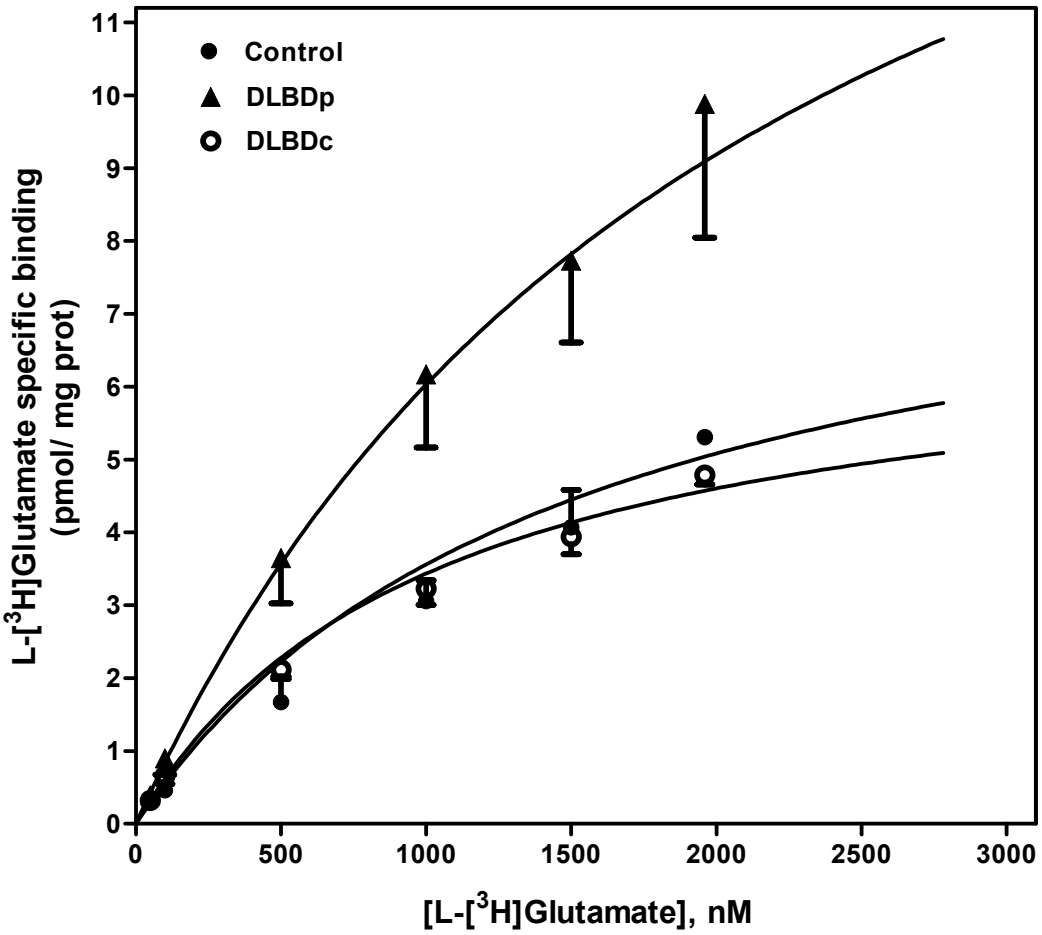

	B_{max} (pmol/mg prot)			K_D (nM)		
Control	8.89 ± 1.16	(5)		1497.5 ± 303.5	(5)	
DLBDp	19.31 ± 1.78	(8)	***	2202.9 ± 430	(6)	**
DLBDc	6.98 ± 0.27	(10)	**	1032.1 ± 108.9	(10)	**

Fig. 2

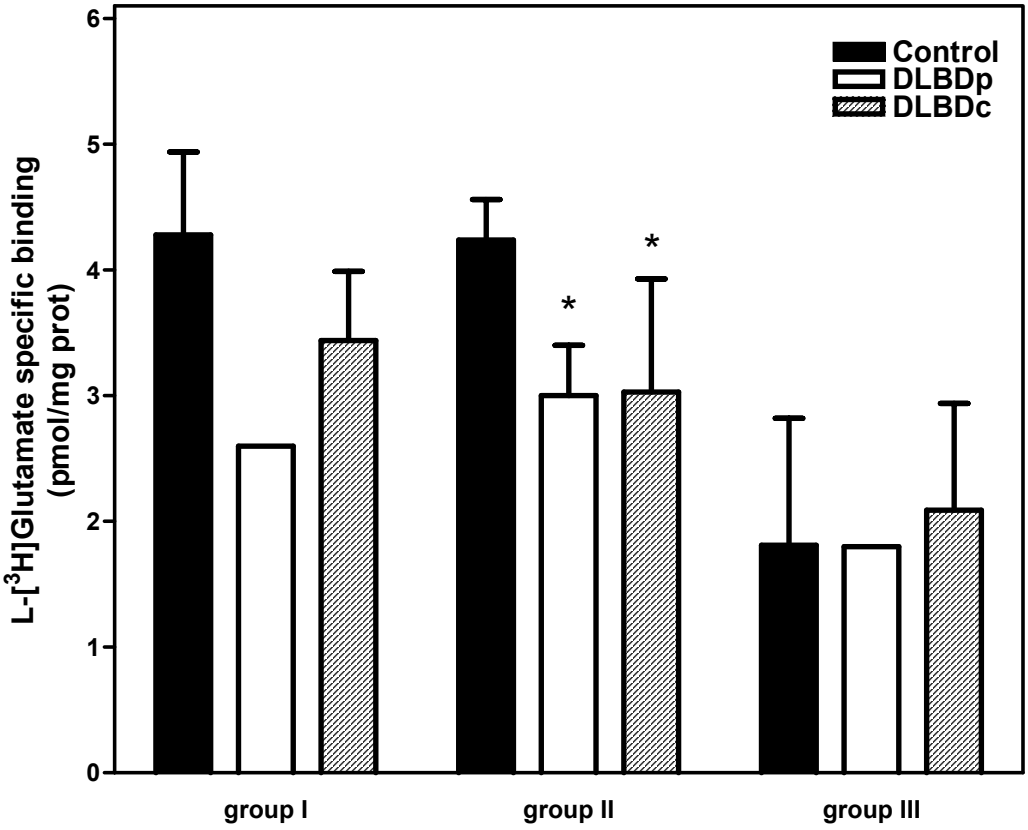
Control
DLBDp
DLBDc
L-[3H]Glutamate specific binding (pmol/mg prot)
0
1
2
3
4
5
6
*
*
group I
group II
group III

Fig. 3

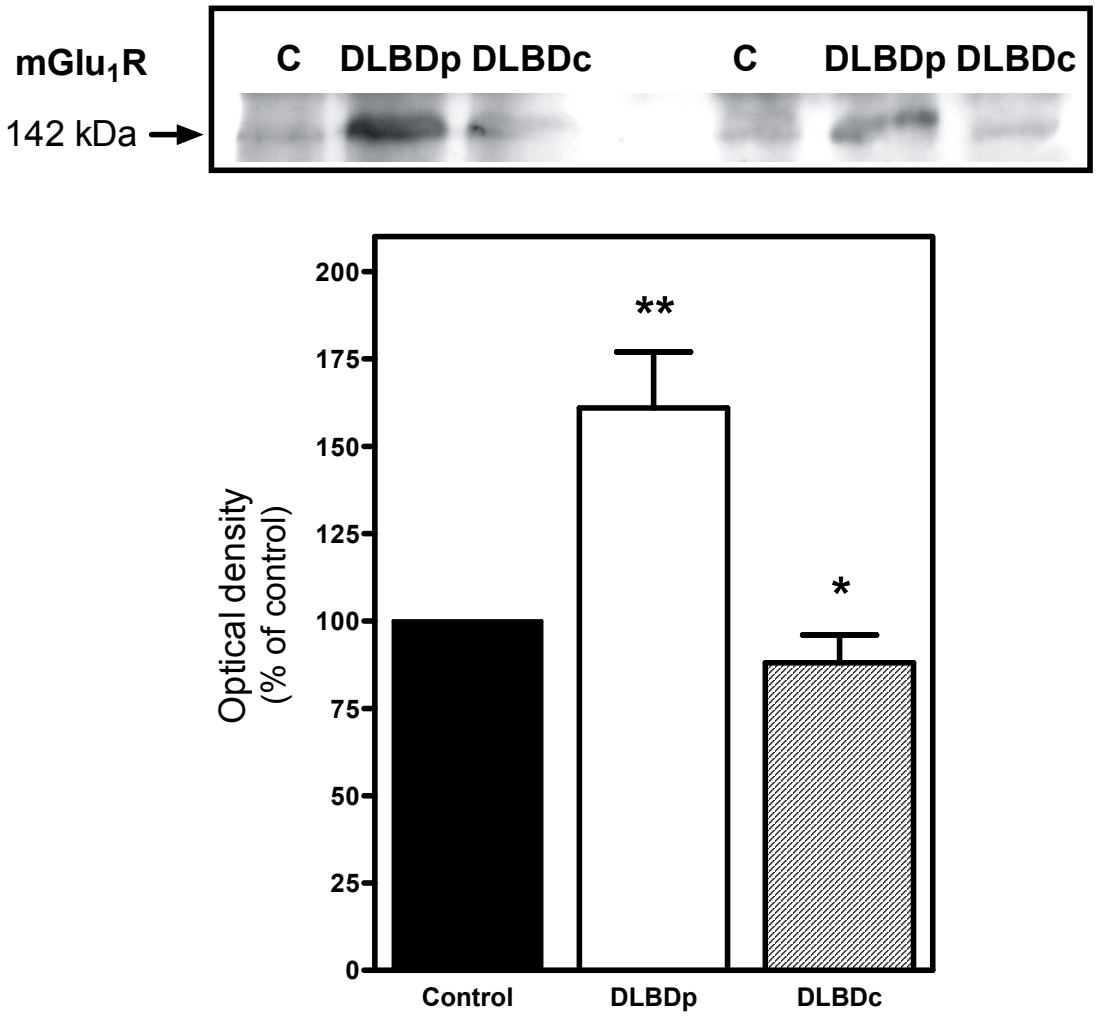
mGlu1R
142 kDa
C
DLBDp
DLBDc
C
DLBDp
DLBDc
Optical density
(% of control)
200
175
150
125
100
75
50
25
0
**
*
Control
DLBDp
DLBDc

Fig. 4

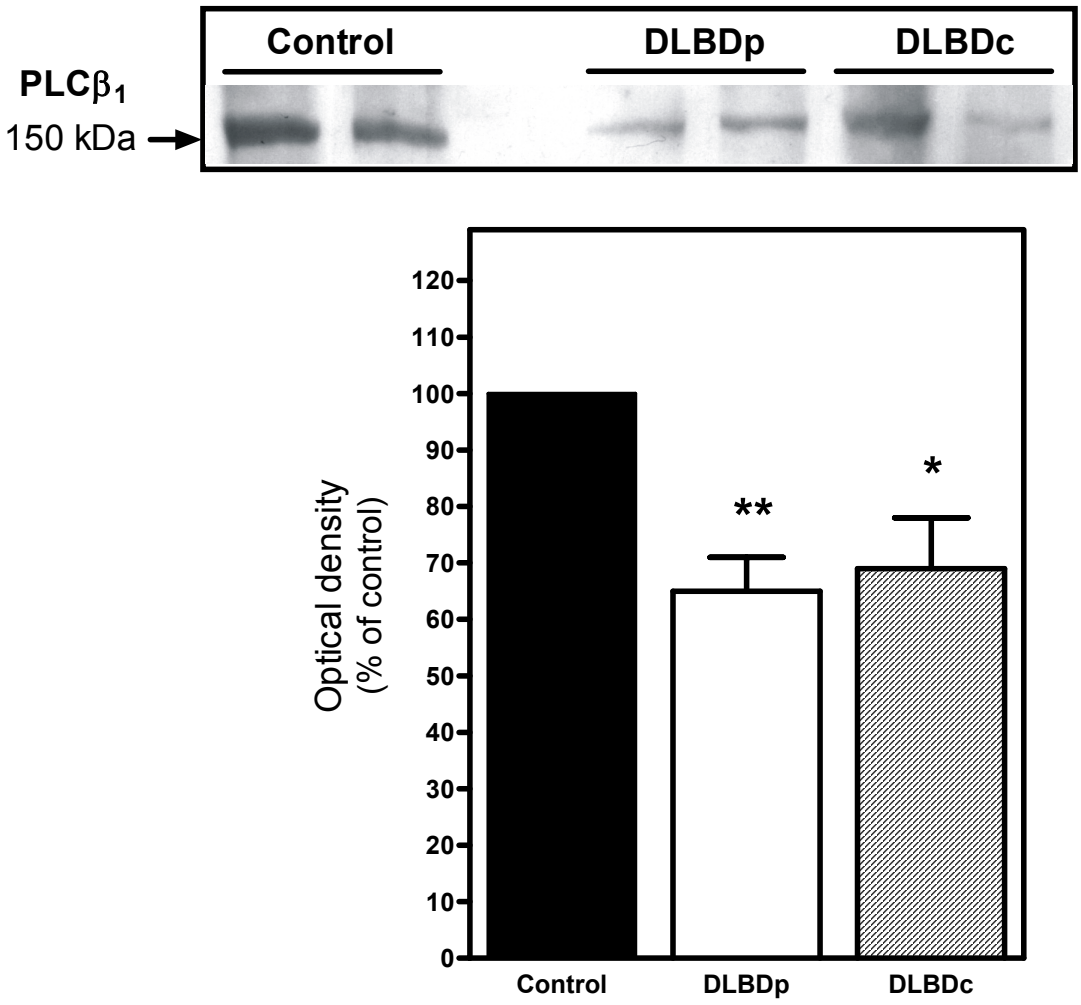
Control
DLBDp
DLBDc
PLCβ1
150 kDa
Optical density
(% of control)
120
110
100
90
80
70
60
50
40
30
20
10
0
**
*
Control
DLBDp
DLBDc

Fig. 5

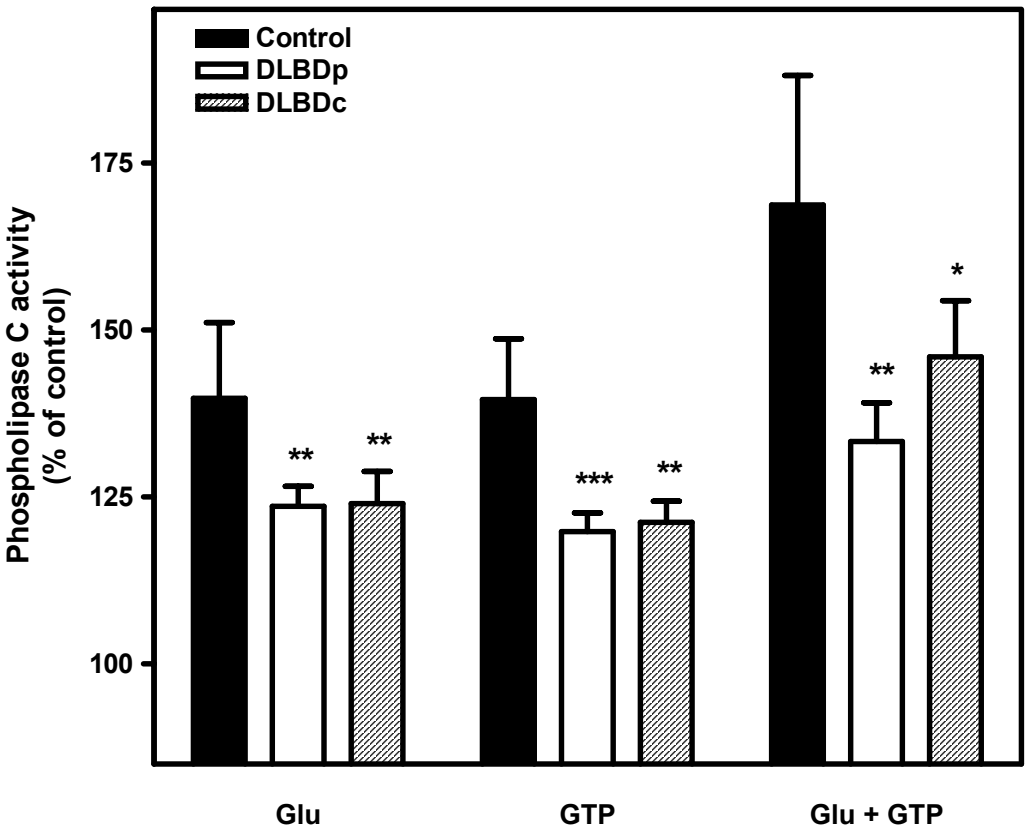
Control
DLBDp
DLBDc
Phospholipase C activity
(% of control)
175
150
125
100
**
**
***
**
**
*
Glu
GTP
Glu + GTP

Fig. 6

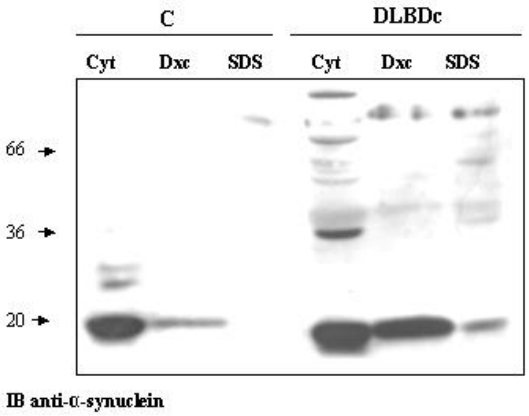

Fig. 7

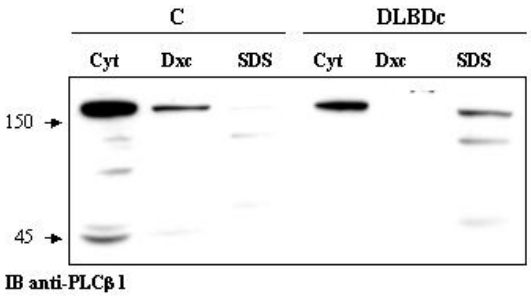

Fig. 8 A

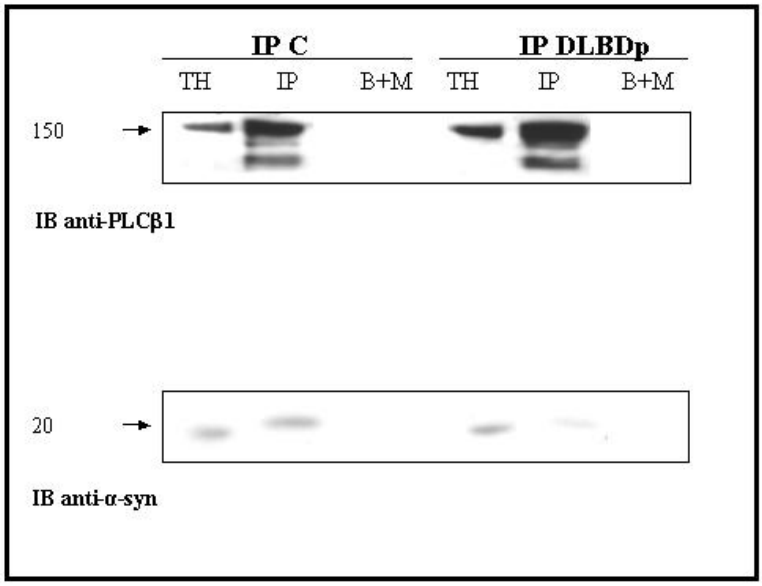

Fig. 8 B

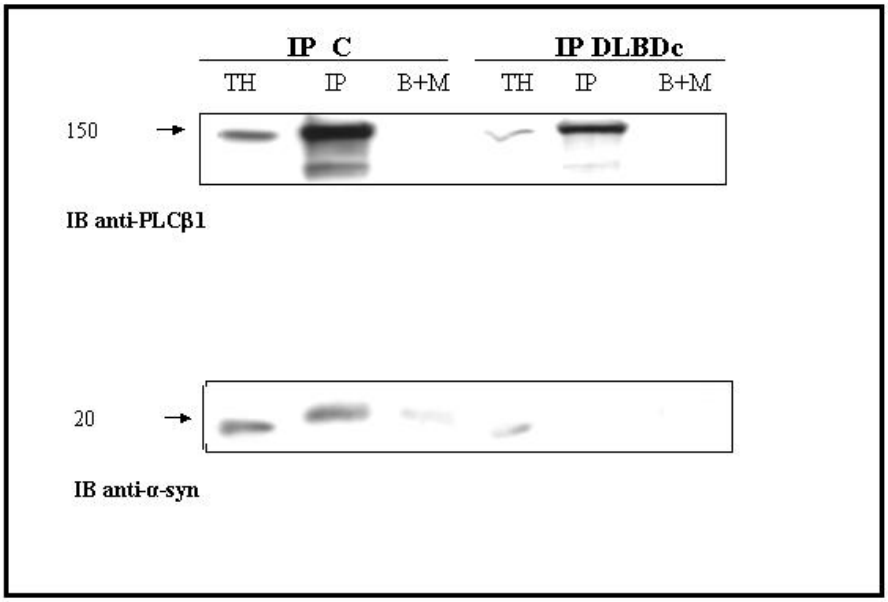

Fig. 9

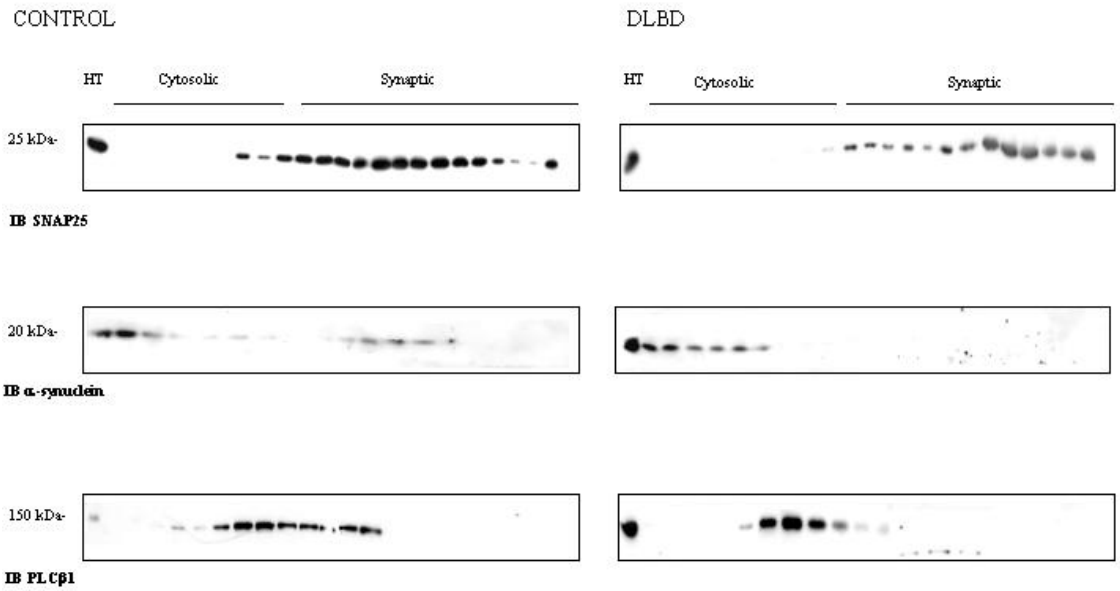
CONTROL
DLBD
HT
Cytosolic
Synaptic
HT
Cytosolic
Synaptic
25 kDa-
IB SNAP25
20 kDa-
IB α-synuclein
150 kDa-
IB PLCβ1

Fig. 10